

SCIENTIFIC REPORTS



OPEN

Inflammatory cytokine IL6 cooperates with CUDR to aggravate hepatocyte-like stem cells malignant transformation through NF- κ B signaling

Qidi Zheng, Zhuojia Lin, Xiaonan Li, Xiaoru Xin, Mengying Wu, Jiahui An, Xin Gui, Tianming Li, Hu Pu, Haiyan Li & Dongdong Lu

Inflammatory cytokines and lncRNAs are closely associated with tumorigenesis. Herein, we reveal inflammatory cytokines IL6 cooperates with long noncoding RNA CUDR to trigger the malignant transformation of human embryonic stem cells-derived hepatocyte-like stem cells. Mechanistically, IL6 cooperates with CUDR to cause MELLT3 to interact with SUV39h1 mRNA 3'UTR and promote SUV39h1 expression. Moreover, the excessive SUV39h1 also increases tri-methylation of histone H3 on ninth lysine (H3K9me3). Intriguingly, under inflammatory conditions, H3K9me3 promotes the excessive expression and phosphorylation of NF- κ B, and in turn, phosphorylated NF- κ B promotes the expression and phosphorylation of Stat3. Furthermore, that the phosphorylated Stat3 loads onto the promoter region of miRs and lncRNAs. Ultimately, the abnormal expression of miRs and lncRNAs increased telomerase activity, telomere length and microsatellite instability (MSI), leading to malignant transformation of hepatocyte-like stem cells.

Human embryonic stem cell lines were differentiated into endoderm-like cells and further differentiated to hepatocyte-like stem cells¹⁻⁴. Because the tumor microenvironment plays a critical role in cancer progression, chronic inflammation is an important process leading to tumorigenesis. Inflammation is often caused by a variety of inflammatory cytokine, e.g. the interleukin (IL)-6, a pleiotrophic cytokine known to be involved in the tumorigenesis⁵. A report indicated Predominant activation of JAK/STAT3 pathway by Interleukin-6 was implicated in hepatocarcinogenesis⁶.

Long non-coding RNAs (lncRNAs) have been shown to have important regulatory roles in cancer biology^{7,8}. Cancer up-regulated drug resistant (Urothelial cancer associated 1, UCA1, CUDR) is a novel non-coding RNA gene which is upregulated in several cancers, such as bladder cancer, breast cancer and colorectal cancer, and plays a pivotal role in cancer progression^{9,10}. In particular, CUDR activates mTOR to regulate hexokinase 2 HK2 through both activation of STAT3 and repression of mir-143^{11,12}. Moreover, CUDR regulates mRNA stability, drug resistance, apoptosis process and Akt signaling pathway¹³⁻¹⁵. Moreover, CUDR regulated cell cycle through CREB via PI3K-AKT dependent pathway in bladder cancer¹⁶, and had important implications in postoperative noninvasive follow-up¹⁷ and during human liver stem cell malignant differentiation^{18,19}. N(6)-methyladenosine (m⁶A) is the most prevalent internal (non-cap) modification present in the messenger RNA of all higher eukaryotes and regulates mRNA stability²⁰. Furthermore, the m(6)A mark acts as a key post-transcriptional modification that promotes the initiation of miRNA biogenesis²¹. In particular, m6A mRNA methylation facilitates resolution of naive pluripotency toward differentiation²². NF- κ B is a key transcriptional regulator involved in inflammation and cell proliferation, survival, and transformation^{23,24}. For example, Metformin suppresses pancreatic tumor growth with inhibition of NF- κ B/STAT3 inflammatory signaling²⁵. Moreover, YM155 potentially triggers cell death in breast cancer cells through an autophagy-NF- κ B network²⁶. In addition, a report indicated that STAT3 could promote epithelial to mesenchymal transition in breast cancer cells²⁷.

School of Life Science and Technology, Tongji University, Shanghai, 200092, China. Correspondence and requests for materials should be addressed to D.L. (email: ludongdong@tongji.edu.cn)

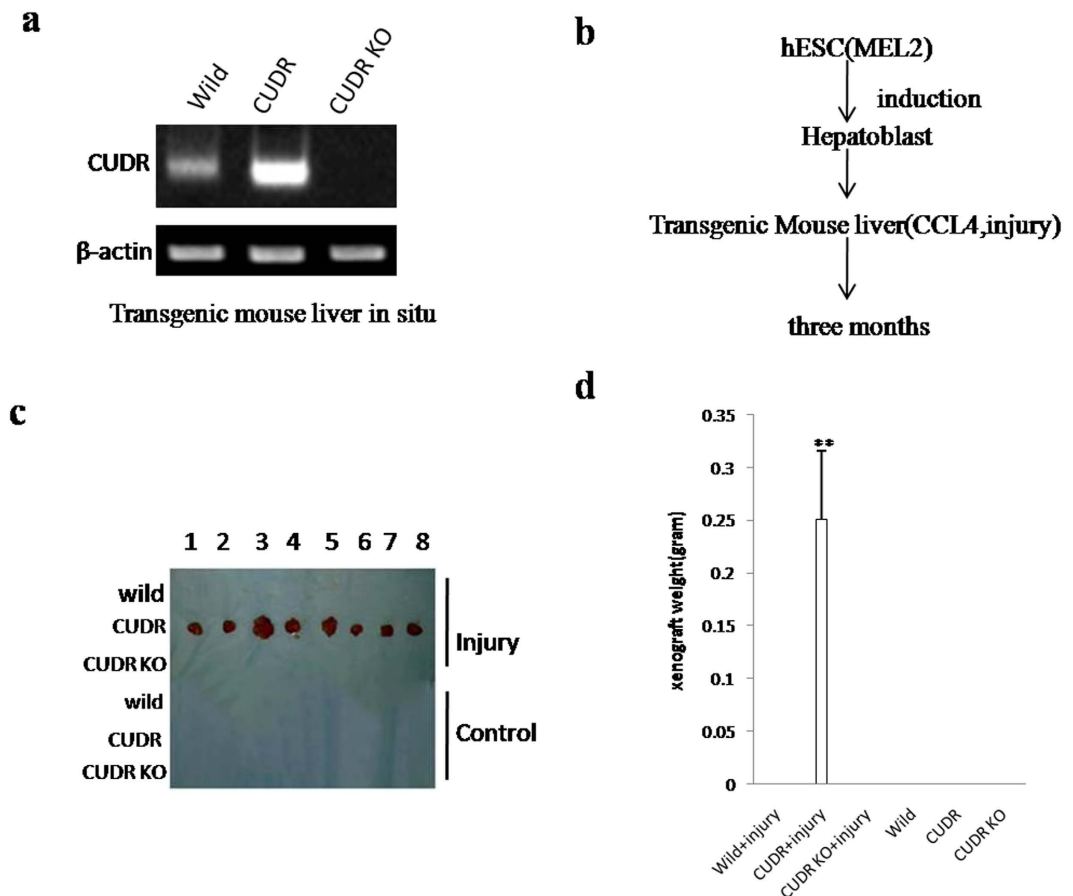


Figure 1. The hepatoblast derived from human ES cells were subjected to transform onto liver cancer in CUDR overexpressed and CCL4 treated injury mouse liver. (a) Mouse liver *in vivo* transfection of CUDR overexpression or knockdown plasmids. The RT-PCR analysis with CUDR primers in these mice liver tissue. β -actin as internal control. (b) The schematic diagram illustrates a model of human stem cell line MEL-2 differentiation into hepatoblast. Then the hepatoblasts were injected into the liver capsule under the B ultrasound guide. CUDR overexpressed/knocked-down and CCL4 induce injury mice Liver *In Vivo* Transfection. (c) The mice were stratified and the tumors were recovered. (d) The wet weight of each tumor was determined for each mouse. Each value was presented as mean \pm standard error of the mean (SEM). ** $P < 0.01$ (b).

In the present study, we demonstrate that interplay between CUDR with inflammatory cytokines prompts the malignant transformation of hepatocyte-like cells induced by human embryonic stem cells. These observations provide insight into a novel link between CUDR and inflammatory cytokines in hepatocarcinogenesis.

Results

CUDR prompts malignant transformation of human embryonic stem cells derived-hepatocyte-like stem cells in mouse injury liver inflammation microenvironment. To explore whether excessive CUDR prompts malignant transformation of human embryonic stem cells derived-hepatocyte-like stem cells in the injury liver inflammation microenvironment induced with Carbon tetrachloride (CCL4), induced hepatotoxicity and trigger liver injury^{28,29}, we performed liver multiple transfection *in vivo* with CUDR overexpression or knockdown plasmids. Compared with wild-type mice, pCMV6-A-GFP-CUDR multiple transfected mouse expressed excessive CUDR, as well as CUDR was knocked down in pGFP-V-RS-CUDR multiple transfected mouse (Fig. 1a). Next, we selected human embryonic stem cells derived- hepatoblasts (HESCDHs) for experiments according to the schematic diagram illustration (Fig. 1b). These HESCDHs were inoculated into the Mouse liver capsule under the B ultrasound guide, including six groups: wild, CUDR, CUDR KO, wild plus CCL4, CUDR plus CCL4, CUDR KO plus CCL4. The CCL4 treatment plus CUDR excessive HESCDHs were transformed into tumor in the mouse injury liver (0.251 ± 0.065 gram, $n = 8$), as well as the tumor was not produced in the rest groups at all (Fig. 1c,d). Furthermore, histological hematoxylin-eosin (HE) staining identified these transformed tumor were malignant liver cancer (Figure S1A). In addition, the AFP (a liver cancer marker) was expressed in the liver tumor tissue (Figure S1B). Taken together, these observations suggest that excessive CUDR can trigger HESCDHs malignant transformation in mouse injury liver inflammatory environment.

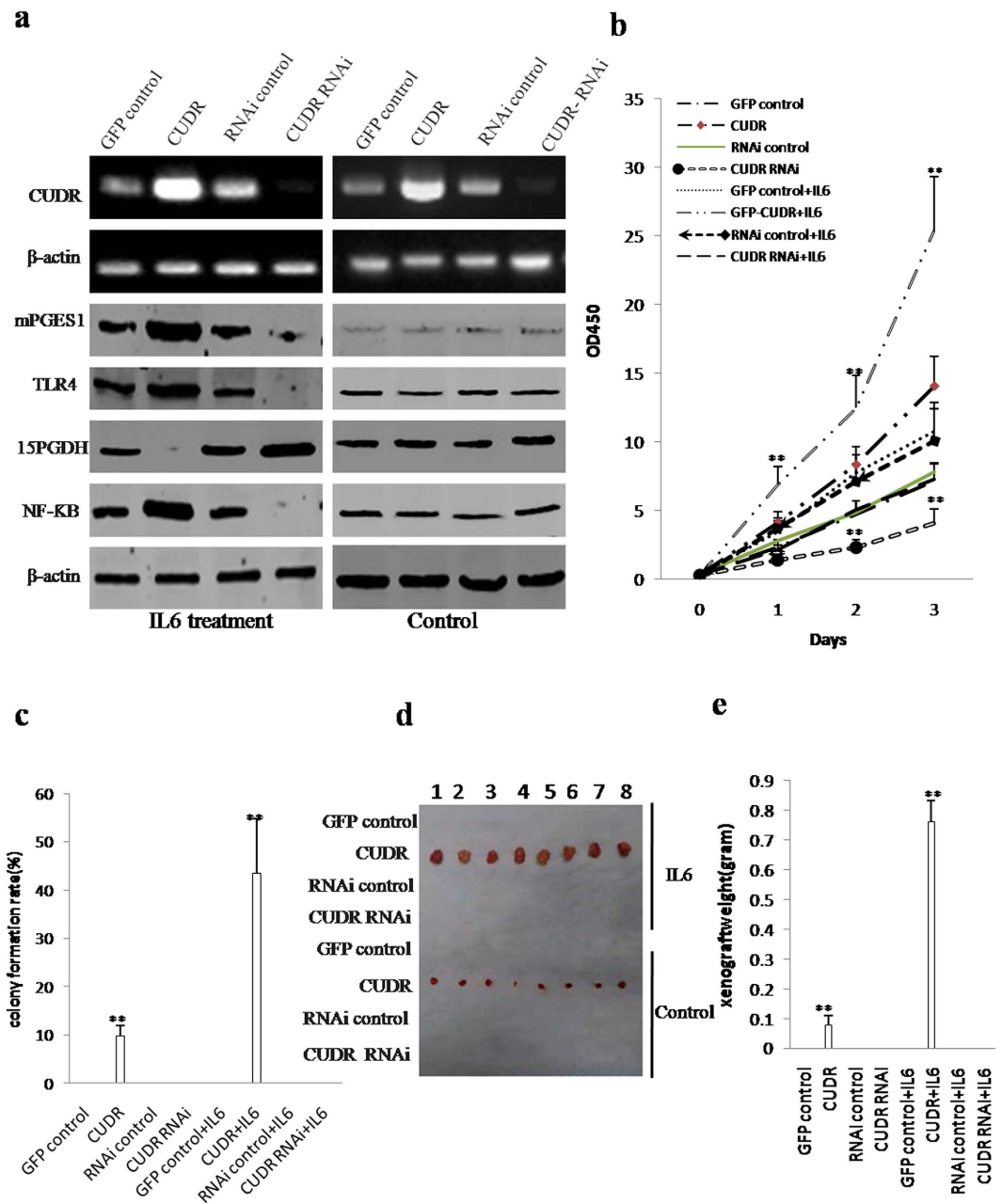


Figure 2. CUDR overexpression combined with inflammatory factor IL6 produced hepatocyte-like stem cells malignant transformation *in vitro* and *in vivo*. (a) RT-PCR analysis for CUDR and Western blotting analysis with anti-mPGES1, anti-TLR4, anti-15PGDH and anti-NF- κ B in the hepatocytes-like stem cells. β -actin as internal control. (b) *In vitro* test in induced and treated hepatocytes-like stem cells. Cells growth assay using CCK8. Each value was presented as mean \pm standard error of the mean (SEM). ** $P < 0.01$. (c) Cells soft agar colony formation assay. (d) *In vivo* test in induced and treated hepatocytes-like stem cells. The mice were stratified and the tumors were recovered. The photography of xenograft tumor in the four groups (indicated in left). (e) The wet weight of each tumor was determined for each mouse. Each value was presented as mean \pm standard error of the mean (SEM), ** $P < 0.01$.

CUDR accelerates hepatocyte-like stem cells malignant transformation in coordination with inflammatory cytokine IL6.

To validate whether the role of CUDR in malignant transformation of hepatocyte-like stem cells needs the help of inflammatory cytokines IL6, we designed the experimental lines (Figure S2A). We first established MEL-2 cell lines with stable overexpression or depletion of CUDR, and induced these transfected MEL-2 cells into hepatoblasts. As shown Fig. 2a, the level of CUDR was increased in pCMV6-A-GFP-CUDR+IL6 (10 μ M) and pCMV6-A-GFP-CUDR group and reduced in pGFP-V-RS-CUDR+IL6 (10 μ M) and pGFP-V-RS-CUDR group compared to control. In IL6 treated groups, excessive CUDR enhanced and CUDR knockdown reduced the mPGES1, TLR4, NF- κ B expression, as well as CUDR overexpression reduced

and CUDR knockdown increased the 15PGDH expression in these induced hepatocyte-like stem cells. On the other hand, mPGES1, TLR4, NF- κ B, 15PGDH expression were significantly not changed in IL6 untreated groups.

Next, we examined the growth curves of the eight hepatocyte-like stem cell lines. As shown in Fig. 2b, in derived hepatocyte-like stem cells treated with IL6, CUDR overexpression significantly increased and CUDR knockdown significantly inhibited the growth of hepatocyte-like stem cells when compared to the control cells. In derived hepatocyte-like stem cells untreated with IL6, CUDR overexpression also significantly increased and CUDR knockdown significantly inhibited the growth of hepatocyte-like stem cells when compared to the control cells. However, this potential role of excessive CUDR was increased in IL6 treated group than in IL6 untreated group. To further address this issue, we detected the S phase cells by BrdU staining. As shown in Figure S2A, after these induced hepatocyte-like stem cells were treated with IL6, excessive CUDR significantly increased ($89.3 \pm 21.3\%$ vs $36.7 \pm 8.4\%$ $p < 0.01$) and CUDR knockdown significantly inhibited ($10.3 \pm 2.1\%$ versus $31.6 \pm 5.2\%$, $p < 0.01$) the BrdU positive rate when compared to the control cells. Although either CUDR overexpression ($54.6 \pm 11.2\%$ versus $23.4 \pm 4.2\%$, $P < 0.05$) or knockdown ($10.3 \pm 2.1\%$ versus $20.1 \pm 3.5\%$, $P < 0.05$) did significantly alter the BrdU positive rate when these derived-hepatocyte-like stem cells were not treated with IL6, the altered capacity was significantly attenuated compared to the IL6 treated hepatocyte-like stem cells. We further performed soft-agar colony formation assay, as shown in Fig. 2c, The soft-agar colony-formation rate was $43.5 \pm 11.2\%$ in the pCMV6-A-GFP-CUDR+IL6 group ($P < 0.01$) and $9.7 \pm 2.2\%$ in the pCMV6-A-GFP-CUDR group ($P < 0.01$), however, the soft-agar colony was not exhibited in the rest groups ($P < 0.01$). Furthermore, the hepatocyte-like stem cells were plated in stem cell conditioned culture medium which allowed for the formation of colonies separated from each other. As shown in Figure S2C, after these derived-hepatocyte-like stem cells were treated with IL6, CUDR overexpression significantly increased ($68.2 \pm 15.3\%$ vs $12.3 \pm 2.7\%$ $p < 0.01$) and CUDR knockdown significantly inhibited ($5.4 \pm 1.2\%$ versus $11.9 \pm 2.4\%$, $p < 0.01$) the self-renewing sphere-formation rate when compared to the control cells. Although either CUDR overexpression ($20.5 \pm 4.2\%$ versus $10.2 \pm 2.1\%$, $P < 0.05$) or knockdown ($4.1 \pm 0.82\%$ versus $8.9 \pm 1.8\%$, $P < 0.05$) did significantly alter the number of self-renewing sphere-formation rate when these derived hepatocyte-like cells were not treated with IL6, the capacity was significantly attenuated compared to that of the IL6 treated hepatocyte-like cells. To further determine whether CUDR plus IL6 promotes hepatocyte-like cells malignant transformation *in vivo* cooperatively, the aforementioned eight group of cell lines were injected subcutaneously at armpit into athymic Balb/C mice. The findings showed that the excessive CUDR and IL6 treated simultaneously hepatocyte-like stem cells were transformed into xenograft tumors (0.76 ± 0.074 gram, $n = 8$, $P < 0.01$) and the excessive CUDR hepatocyte-like stem cells also were transformed into xenograft tumors (0.0775 ± 0.032 gram, $n = 8$, $P < 0.01$), as well as the xenograft tumor was not appeared in the rest groups at all (Fig. 2d,e). Furthermore, pathological examination (H&E staining) of the xenograft tumors revealed a poorly-differentiated tumor cells (Figure S2D). Taken together, CUDR combined with IL6 collaboratively aggravates derived-hepatocyte-like stem cells malignant transformation and proliferation.

CUDR enhances the expression of suppressor of variegation 3–9 homolog 1 (SUV39H1), a histone methyltransferase, dependent on IL6.

To elucidate whether CUDR may enhance SUV39h2 expression via IL6, we first performed Chromatin Immunoprecipitation (CHIP) to detect the transcriptional activity of SUV39h2. As shown in Fig. 3a, CUDR overexpression facilitated and CUDR knockdown reduced the loading of CREPT ((cell-cycle related and expression-elevated protein in tumor) and RNA polymerase II onto the SUV39h2 promoter region. Moreover, CUDR overexpression increased and CUDR knockdown decreased the SUV39h2 promoter luciferase activity (Fig. 3b). Furthermore, CUDR overexpression enhanced and CUDR knockdown inhibited the METTL3 expression. However, CUDR overexpression or knockdown did not alter the FTO expression in IL6 treated hepatocyte-like cells (Figure S3A). Intriguingly, RNA Immunoprecipitation (RIP) with anti-METTL3 showed that CUDR overexpression enhanced and CUDR knockdown inhibited the binding of METTL3 to SUV39h2 mRNA (Fig. 3c). Furthermore, RNA Immunoprecipitation (RIP) with anti-N6Ame showed that CUDR overexpression enhanced and CUDR knockdown inhibited the mRNA methylation of SUV39h2 (Fig. 3d). Super-EMSA (gel-shift) (Figure S3B) and Nuclear Run-on assay (Figure S3C) also identified that CUDR overexpression enhanced and CUDR knockdown inhibited the mRNA methylation of SUV39h2 in IL6 treated hepatocyte-like cells. Moreover, RT-PCR findings showed that CUDR overexpression enhanced and CUDR knockdown inhibited SUV39h2 mRNA expression (Fig. 3e). Finally, western blotting and IP results showed that CUDR overexpression enhanced and CUDR knockdown inhibited the expression, phosphorylation and sumoylation of SUV39h2 (Fig. 3f). Collectively, CUDR enhances the expression and modification of SUV39h2 in IL6 treated hepatocyte-like stem cells on the transcriptional and post-transcriptional level (mRNA methylation modification).

CUDR cooperates with IL6 to enhance expression and phosphorylation of NF- κ B through SUV39h2 in the inflammatory environment.

Activated NF- κ B translocates into the nucleus and stimulates the expression of genes involved in a wide variety of biological functions. To validate whether CUDR combined with IL6 could enhance the expression and phosphorylation of NF- κ B, we performed Co-Immunoprecipitation (IP), Western blotting, Chromosome conformation capture (3C)-chromatin immunoprecipitation (ChIP), promoter luciferase activity assay and RT-PCR in IL6 treated hepatocyte-like stem cells transfected with pCMV6-A-GFP, pCMV6-A-GFP-CUDR, pGFP-V-RS, pGFP-V-RS-CUDR. As shown in Fig. 4a, CUDR overexpression promoted and CUDR knockdown inhibited the interplay between SUV39h2 and Histone H3. CUDR overexpression promoted and CUDR knockdown inhibited the modifications of mono-, double-, tri-methylation on the ninth lysine of Histone 3 (H3K9me1, H3K9me2, H3K9me3) (Fig. 4b). Furthermore, CUDR overexpression promoted and CUDR knockdown inhibited NF- κ B promoter-enhancer DNA loop formation and blocked the H3K9me3, RNA polymerase II entering into the loop in these IL6 treated hepatocyte-like

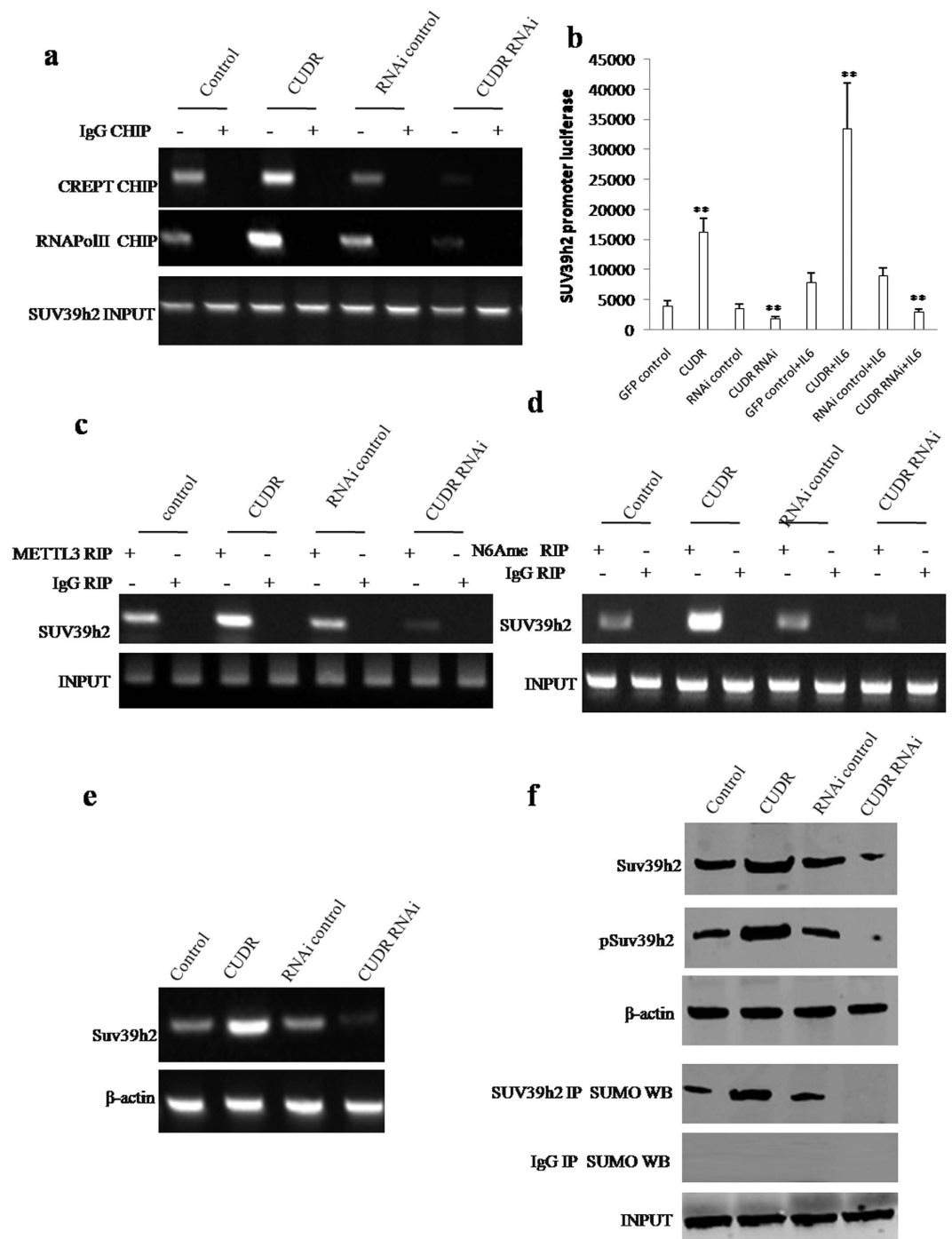


Figure 3. CUDR enhances SUV39h2 expression in hepatocyte-like stem cells with IL6 treatment. (a) Chromatin Immunoprecipitation (CHIP) with anti-CREPT, anti-RNA PolII followed by PCR with SUV39h2 promoter primers in hepatocyte-like stem cells treated with IL6 and transfected with pCMV6-A-GFP, pCMV6-A-GFP-CUDR, pGFP-V-RS, pGFP-V-RS-CUDR. IgG CHIP as negative control. SUV39h2 promoter DNA as INPUT. (b) SUV39h2 promoter luciferase activity assay. Each value was presented as mean \pm standard error of the mean (SEM). ** $P < 0.01$. (c) RNA Immunoprecipitation (RIP) with anti-METTL3 followed by RT-PCR with SUV39h2 primers. IgG RIP as negative control. SUV39h2 mRNA as INPUT. (d) RNA Immunoprecipitation (RIP) with anti-N6Ame followed by RT-PCR with SUV39h2 mRNA primers. IgG RIP as negative control. SUV39h2 mRNA as INPUT. (e) SUV39h2 expression analysis by RT-PCR. β -actin as internal control. (f) The analysis of SUV39h2 expression, SUV39h2 phosphorylation and SUV39h2 sumoylation by western blotting with anti-SUV39h2, anti-pSUV39h2, β -actin as internal control, or IP with anti-SUV39h2 and anti-SUMO western blotting. Western blotting with anti-SUV39h2 was used as INPUT.

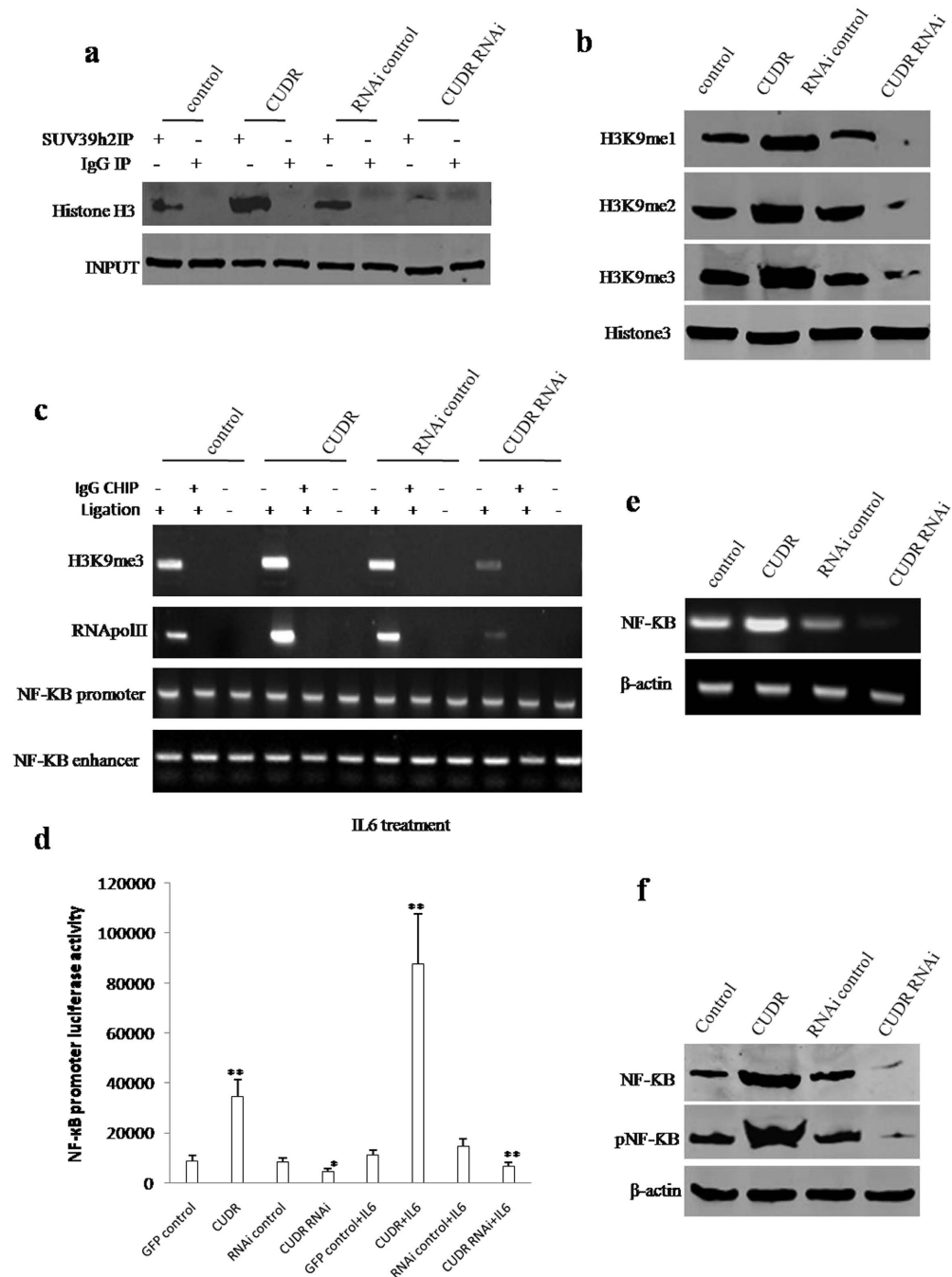


Figure 4. CUDR cooperates with IL6 to enhance the expression and phosphorylation of NF- κ B. (a) Anti-SUV39h2 Co-Immunoprecipitation (IP) followed by western blotting with anti-Histone H3 in hepatocyte-like cells treated with IL6 and transfected with pCMV6-A-GFP, pCMV6-A-GFP-CUDR, pGFP-V-RS, pGFP-V-RS-CUDR. IgG IP as negative control. INPUT refers to western blotting with anti-Suv39h2. (b) Western blotting with anti-H3K9me1, anti-H3K9me2, anti-H3K9me3 in IL6 treated hepatocyte-like cells transfected with pCMV6-A-GFP, pCMV6-A-GFP-CUDR, pGFP-V-RS, pGFP-V-RS-CUDR. Histone3 as internal control. (c) Chromosome conformation capture (3C)-chromatin immunoprecipitation (ChIP) with anti-H3K9me3, anti-RNA polII in hepatocyte-like cells treated with IL6 and transfected with pCMV6-A-GFP, pCMV6-A-GFP-CUDR, pGFP-V-RS, pGFP-V-RS-CUDR. The chromatin is cross-linked, digested with restriction enzymes, and ligated under conditions that favor intramolecular ligation. Immediately after ligation, the chromatin is immunoprecipitated using an antibody (anti-H3K9me3, anti-RNA polII) against the protein of interest. Thereafter, the cross-links are reversed, and the DNA is purified further. The PCR analysis is applied for detecting NF- κ B promoter-enhancer coupling product using NF- κ B promoter and enhancer primers. The NF- κ B promoter and enhancer as INPUT. (d) NF- κ B promoter luciferase activity assay. Each value was presented as mean \pm standard error of the mean (SEM), ** $P < 0.01$. (e) The analysis of NF- κ B expression by RT-PCR with NF- κ B primers. β -actin as internal control. (f) Western blotting with anti-NF κ B and anti-pNF κ B. β -actin as internal control.

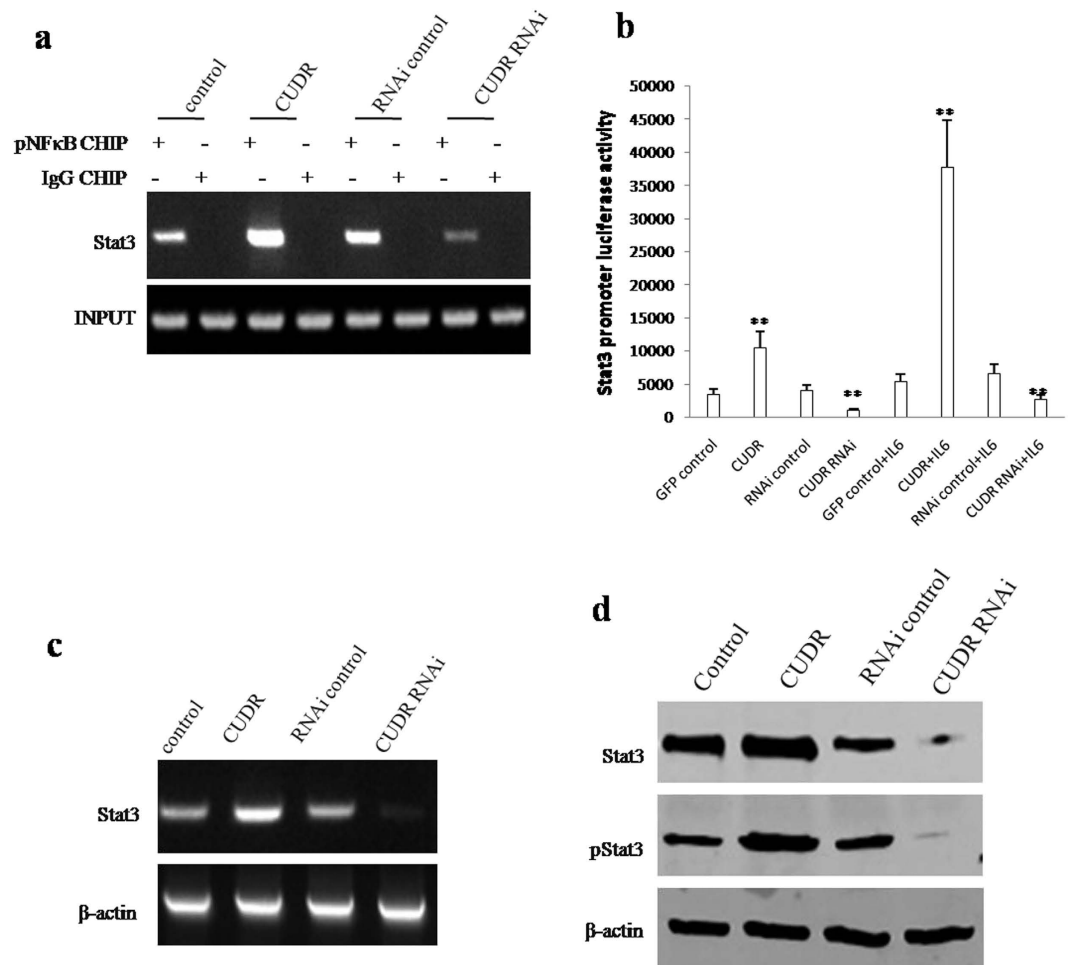


Figure 5. CUDR plus IL6 enhances Stat3 expression and phosphorylation through pNF-κB. (a) Chromatin Immunoprecipitation (CHIP) with anti- pNF-κB followed by PCR with Stat3 promoter primers in hepatocyte-like stem cells treated with IL6 and transfected with pCMV6-A-GFP, pCMV6-A-GFP-CUDR, pGFP-V-RS, pGFP-V-RS-CUDR. IgG CHIP as negative control. Stat3 promoter DNA as INPUT. (b) Stat3 promoter luciferase activity assay. Each value was presented as mean ± standard error of the mean (SEM). **P < 0.01. (c) The analysis of Stat3 expression by RT-PCR with Stat3 primers. β-actin as internal control. (d) Western blotting with anti-Stat3 and pStat3 in hepatocyte-like stem cells treated with IL6 and transfected with pCMV6-A-GFP, pCMV6-A-GFP-CUDR, pGFP-V-RS, pGFP-V-RS-CUDR. β-actin as internal control.

cells (Fig. 4c). However, this action was abrogated when these hepatocyte-like cells were not treated with IL6 (Figure S4). Moreover, the luciferase activity assay showed that CUDR overexpression promoted and CUDR knockdown inhibited NFκB promoter luciferase activity in these IL6 treated hepatocyte-like cells (Fig. 4d). RT-PCR results showed CUDR overexpression promoted and CUDR knockdown inhibited NFκB transcription in these IL6 treated hepatocyte-like stem cells (Fig. 4e). Western blotting showed CUDR overexpression promoted and CUDR knockdown inhibited the expression and its phosphorylation of NFκB in these IL6 treated hepatocyte-like stem cells (Fig. 4f). Collectively, these observations suggest that CUDR enhances the expression and phosphorylation of NFκB in IL6 treated hepatocyte-like stem cells.

CUDR plus IL6 enhances the expression and phosphorylation of Stat3 through pNF-κB. To address whether CUDR altered the expression and its phosphorylation of Stat3 through NFκB, we first performed the Chromatin Immunoprecipitation (CHIP) assay in hepatocyte-like stem cells treated with IL6 and transfected with pCMV6-A-GFP, pCMV6-A-GFP-CUDR, pGFP-V-RS, pGFP-V-RS-CUDR. As show in the Fig. 5a, excessive CUDR enhanced and CUDR knockdown inhibited the pNFκB occupancy on the Stat3 promoter region. However, in hepatocyte-like stem cells untreated with IL6, neither CUDR overexpression nor CUDR knockdown did significantly alter the pNFκB occupancy on the Stat3 promoter region (**data not shown**). Moreover, excessive CUDR increased and CUDR knockdown reduced the Stat3 promoter luciferase activity in hepatocyte-like stem cells treated with IL6 (Fig. 5b). Therefore, excessive CUDR promotes and CUDR knockdown inhibited the transcription (Fig. 5c), translation and phosphorylation (Fig. 5d) of Stat3 in hepatocyte-like cells treated with IL6.

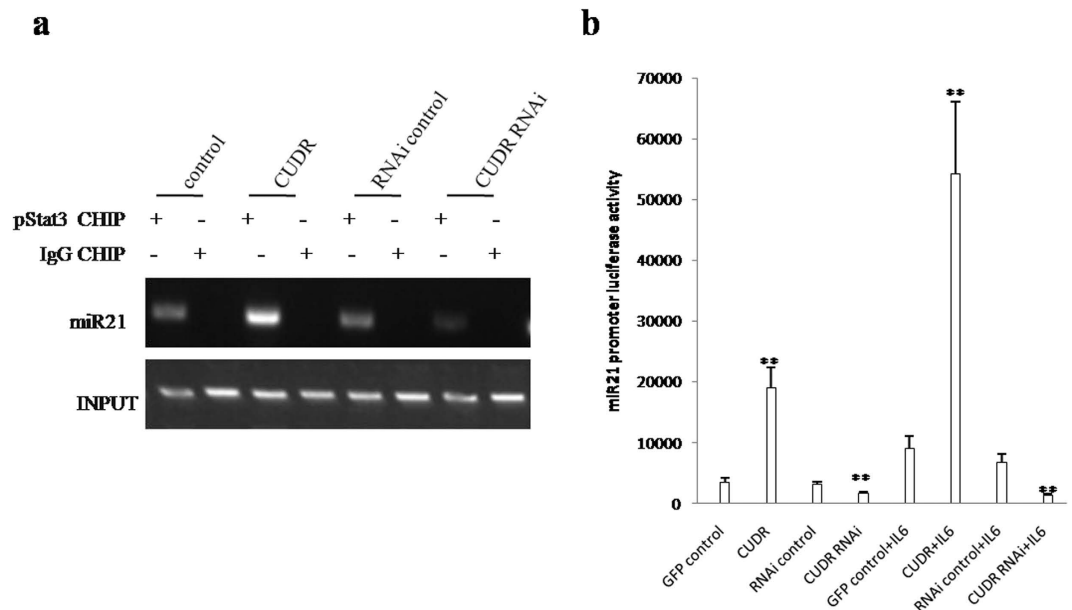


Figure 6. CUDR plus IL6 promotes miRs expression through pStat3. (a) Chromatin Immunoprecipitation (CHIP) with anti-pStat3 followed by PCR with miR21 promoter primer in hepatocyte-like cells treated with and without IL6 transfected with pCMV6-A-GFP, pCMV6-A-GFP-CUDR, pGFP-V-RS, pGFP-V-RS-CUDR. IgG CHIP as negative control. miR21 promoter DNA as INPUT. (b) miR21 promoter luciferase activity assay. Each value was presented as mean \pm standard error of the mean (SEM). ** $P < 0.01$.

Together, these observations suggest that excessive CUDR cooperates with IL6 to enhance the expression and phosphorylation of Stat3 dependent on NF- κ B phosphorylation.

CUDR prompts to alter the expression of microRNAs and lncRNAs through pStat3 in the inflammatory environment.

To elucidate whether CUDR alters the expression of microRNAs and lncRNAs through pStat3 under the inflammatory condition, we first performed Chromatin immunoprecipitation (CHIP) with anti-pStat3 followed by PCR with miR21, miR155, miR17, miR675, miR372, miR192 promoter primers in IL6 treated hepatocyte-like cells transfected with pCMV6-A-GFP, pCMV6-A-GFP-CUDR, pGFP-V-RS, pGFP-V-RS-CUDR. As shown in Figs 6a and S5A, excessive CUDR enhanced and CUDR knockdown inhibited the loading of pStat3 on the promoter region of miR21, miR155, miR17, miR675, miR372, miR192. Excessive CUDR increased and CUDR knockdown decreased the miR21, miR155, miR17, miR675, miR372, miR192 promoter luciferase activity (Fig. 6b). Nuclear run on assay showed that excessive CUDR enhanced and CUDR knockdown inhibited the expression of miR21, miR155, miR17, miR675, miR372, miR192 (Figure S5B). Furthermore, excessive CUDR enhanced and CUDR knockdown inhibited the loading of pStat3 on the promoter region of CUDR, HOTAIR, MALAT1, HULC, H19. Excessive CUDR inhibited and CUDR knockdown enhanced the loading of pStat3 on the promoter region of MEG3, TERRA (Figs 7a and S6). Strikingly, excessive CUDR increased and CUDR knockdown decreased the methylation on promoter regions of TERRA (Fig. 7a) and MEG3 (Fig. 7b). Moreover, excessive CUDR decreased and CUDR knockdown increased the TERRA promoter luciferase activity (Fig. 7c). Furthermore, Nuclear Run-on assay showed that excessive CUDR promoted and CUDR knockdown inhibited the expression of CUDR, HOTAIR, MALAT1, HULC, H19, as well as excessive CUDR inhibited and CUDR knockdown increased the expression of MEG3 and TERRA (Fig. 7d). Moreover, RT-PCR results showed that CUDR promoted and CUDR knockdown inhibited the expression of CUDR, HOTAIR, MALAT1, HULC, H19, as well as excessive CUDR inhibited and CUDR knockdown increased the expression of MEG3 and TERRA (Fig. 7e). Taken Together, these observations suggest that CUDR prompts to alter the expression of microRNAs and lncRNAs dependent on pStat3 in IL6 treated hepatocyte-like stem cells.

CUDR cooperates with IL6 to enhance telomerase activity, elongate telomere length and increase microsatellite instability (MSI).

Given that CUDR inhibits the TERRA expression which can inhibit TERT activity, we had to consider whether CUDR impacted on telomerase activity, telomere length and microsatellite instability (MSI). In hepatocyte-like cells with IL6 treatment plus CUDR overexpression or depletion, RNA Immunoprecipitation (RIP) with anti-TERT showed that excessive CUDR increased and CUDR knockdown inhibited the interplay between TERT and TERC, as well as excessive CUDR inhibited and CUDR knockdown increased the interplay between TERT and TERRA (Fig. 8a). Excessive CUDR increased and CUDR knockdown inhibited the telomerase activity in hepatocyte-like stem cells with IL6 treatment. However, both excessive CUDR and CUDR knockdown did significantly not alter the telomerase activity in hepatocyte-like stem cells without IL6 treatment (Fig. 8b). The regular PCR detection of telomere repeat sequence in hepatocyte-like cells with IL6 treatment showed that excessive CUDR increased and CUDR knockdown decreased the telomere

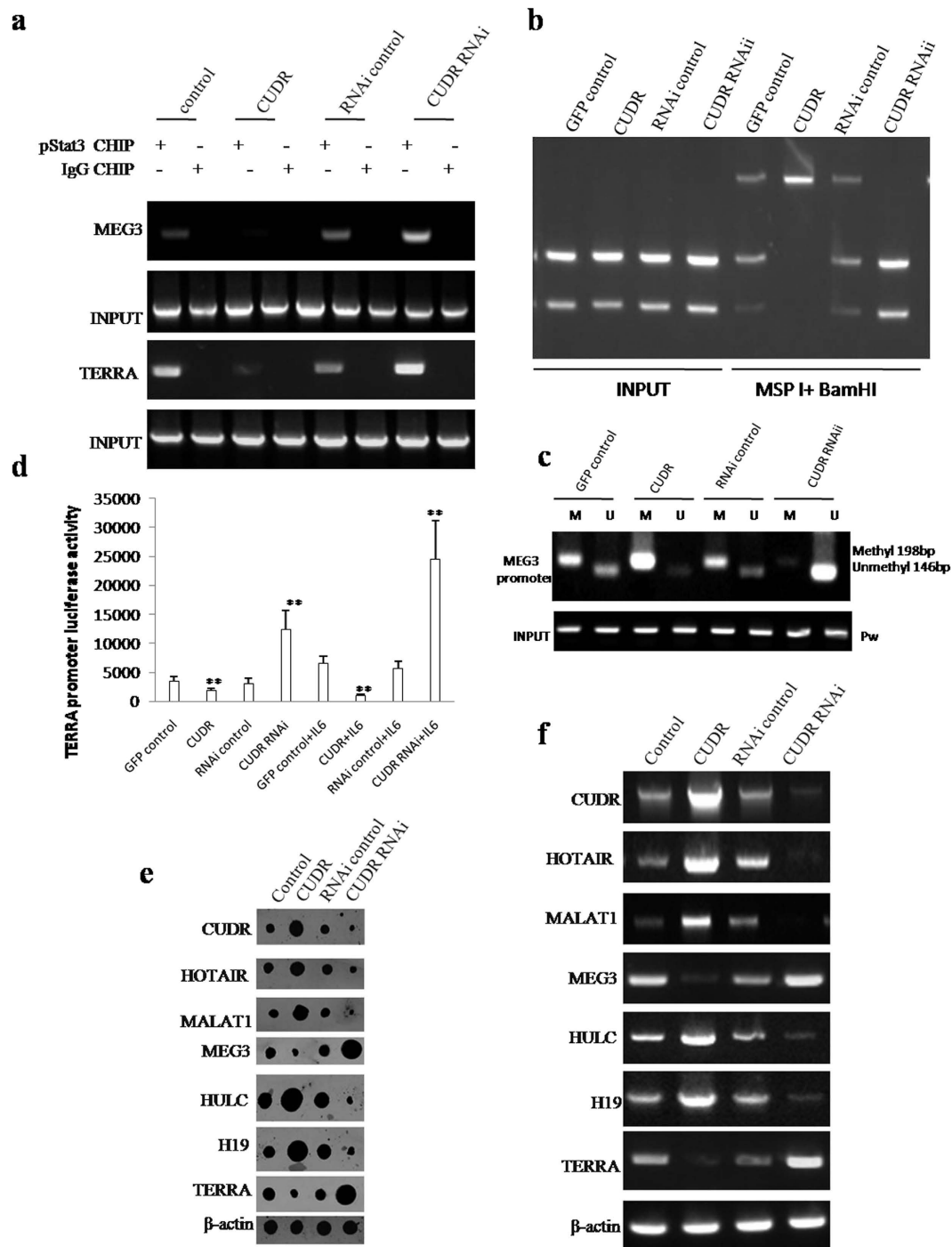


Figure 7. CUDR plus IL6 alters long noncoding RNA expression through pStat3. (a) Chromatin Immunoprecipitation (CHIP) with anti- pStat3 followed by PCR with MEG3, TERRA promoter primer in hepatocyte-like cells treated with IL6 and transfected with pCMV6-A-GFP, pCMV6-A-GFP-CUDR, pGFP-V-RS, pGFP-V-RS-CUDR. IgG CHIP as negative control. MEG3, TERRA promoter DNA as INPUT. (b) (a) TERRA promoter methylation analysis by MspI plus BamHI digestion in hepatocyte-like cells treated with and transfected with pCMV6-A-GFP, pCMV6-A-GFP-CUDR, pGFP-V-RS, pGFP-V-RS-CUDR. (b) MEG3 promoter methylation analysis with MSP method primer in hepatocyte-like cells treated with IL6 and transfected with pCMV6-A-GFP, pCMV6-A-GFP-CUDR, pGFP-V-RS, pGFP-V-RS-CUDR. (c) CUDR, HOTAIR, MALAT1, MEG3, HULC, H19, TERRA promoter luciferase activity assay. Each value was presented as mean \pm standard error of the mean (SEM). ** $P < 0.01$. (d) Nuclear run on analysis with Biotin probe of CUDR, HOTAIR, MALAT1, MEG3, HULC, H19, TERRA in hepatocyte-like cells treated with IL6 and transfected with pCMV6-A-GFP, pCMV6-A-GFP-CUDR, pGFP-V-RS, pGFP-V-RS-CUDR. β -actin as internal control. (e) RT-PCR analysis with Biotin probe of CUDR, HOTAIR, MALAT1, MEG3, HULC, H19, TERRA in hepatocyte-like stem cells treated with IL6 and transfected with pCMV6-A-GFP, pCMV6-A-GFP-CUDR, pGFP-V-RS, pGFP-V-RS-CUDR. β -actin as internal control.

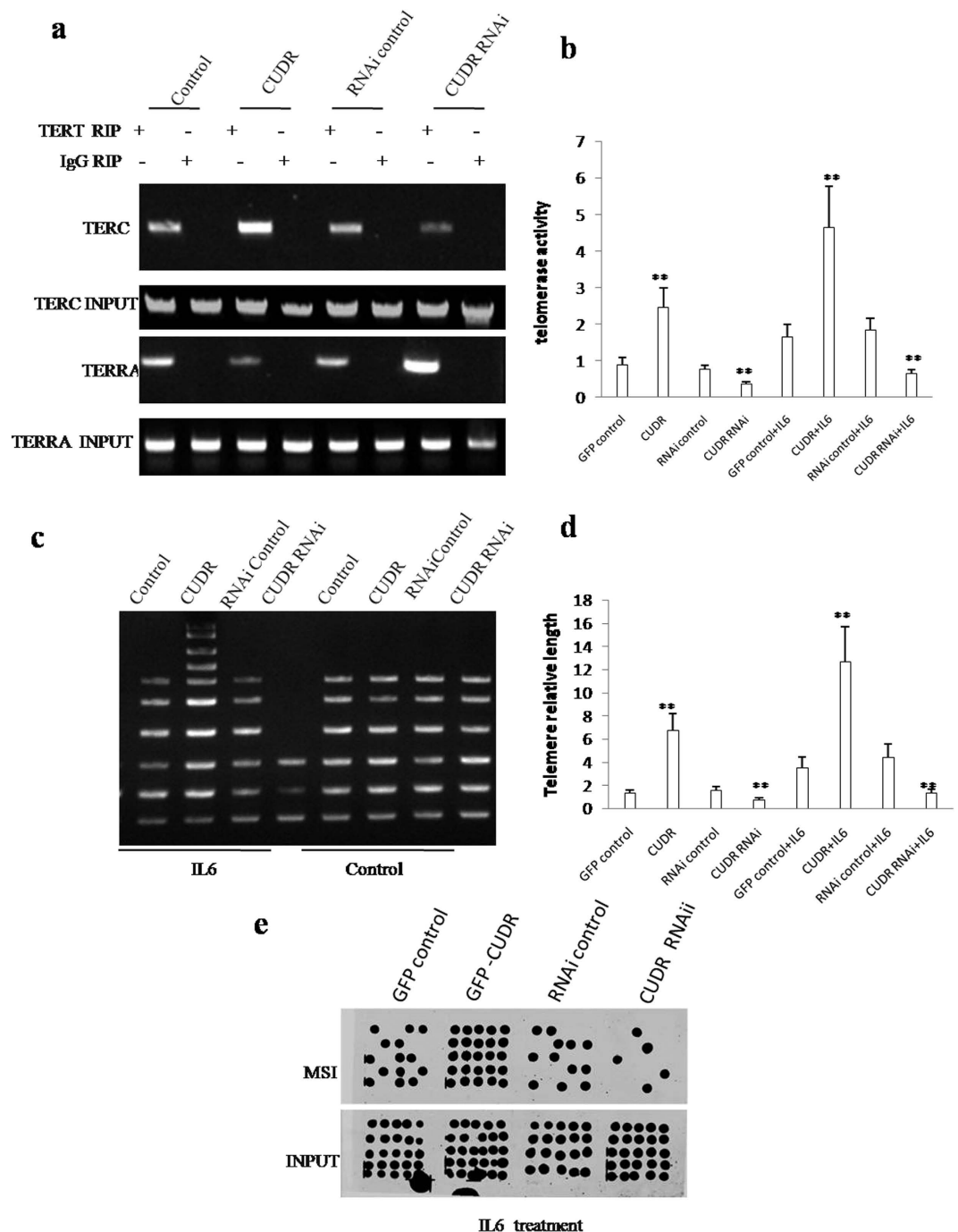


Figure 8. CUDR plus IL6 enhanced telomerase activity, elongates telomere length and increased Microsatellite Instability (MSI) in CUDR overexpressing hepatocyte-like cells treated with IL6. (a) RNA Immunoprecipitation (CHIP) with anti-TERT followed by RT-PCR with TERC and TERRA RNA primers in hepatocyte-like cells treated with IL6 and transfected with pCMV6-A-GFP, pCMV6-A-GFP-CUDR, pGFP-V-RS, pGFP-V-RS-CUDR. IgG CHIP as negative control. TERC and TERRA promoter DNA as INPUT. (b) Telomerase activity assay with TRAP method. (c) The PCR detection of telomere repeat sequence in IL6 treated hepatocyte-like stem cells transfected with pCMV6-A-GFP, pCMV6-A-GFP-CUDR, pGFP-V-RS, pGFP-V-RS-CUDR. (d) The real-time PCR detection of telomere length. Each value was presented as mean \pm standard error of the mean (SEM). ** $P < 0.01$. (e) Microsatellite Instability (MSI) analysis through Dot blot (Slot blot) using various Biotin labelling MSI probes (Biotin-MSIs) in hepatocyte-like cells treated with IL6 and transfected with pCMV6-A-GFP, pCMV6-A-GFP-CUDR, pGFP-V-RS, pGFP-V-RS-CUDR.

length. However, this action was abrogated in control group (Fig. 8c). The real-time PCR detection of telomere repeat sequence in hepatocyte-like stem cells with IL6 treatment showed that excessive CUDR increased and

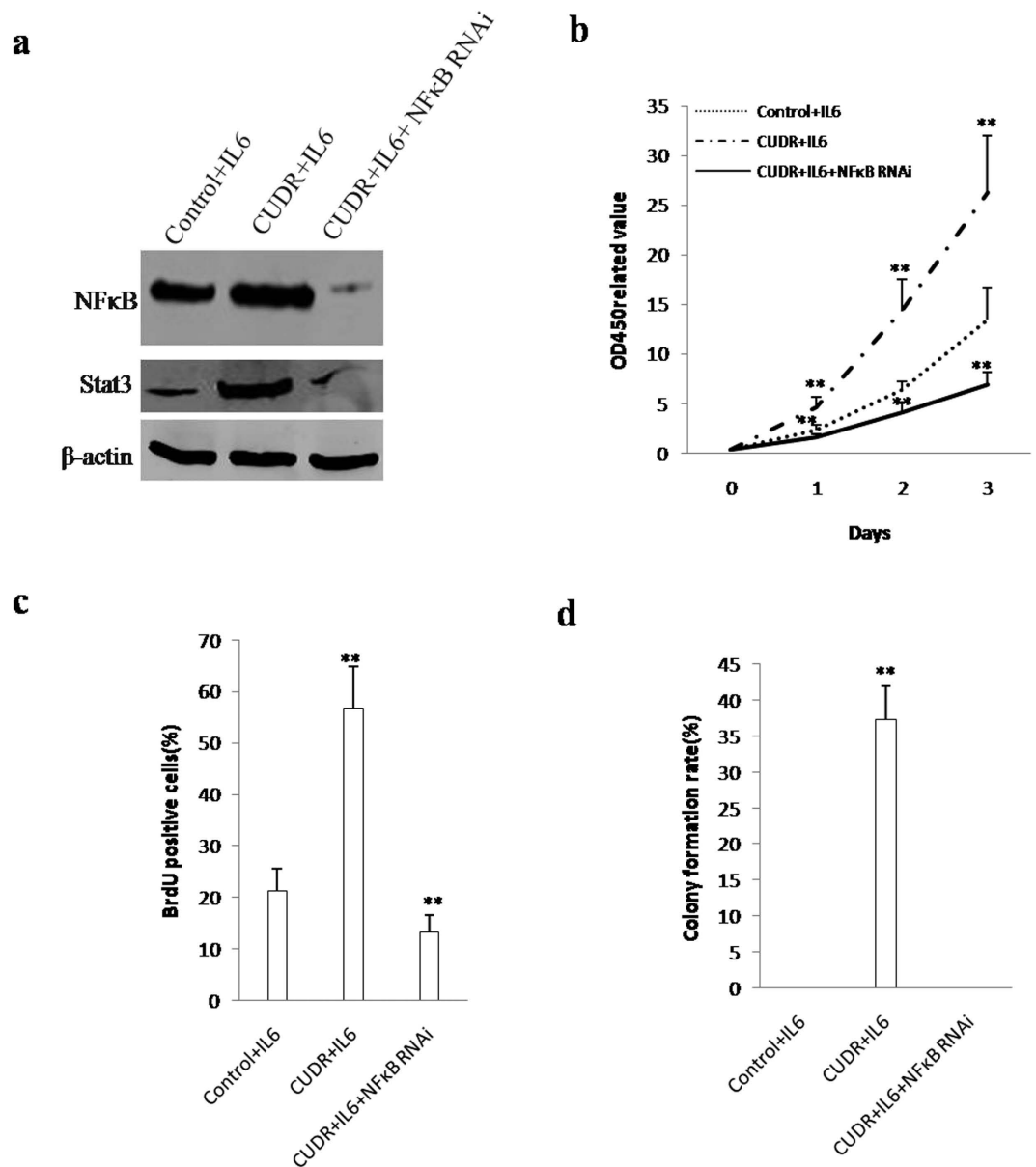


Figure 9. IL6 cooperates with CUDR to aggravate hepatocyte-like stem cells malignant transformation through NF- κ B signaling. (a) Western blotting analysis with anti- NF- κ B, anti-Stat3 in the hepatocytes-like stem cells. β -actin as internal control. (b) Cells growth assay using CCK8. Each value was presented as mean \pm standard error of the mean (SEM). **P < 0.01. (c) BrdU assay in the hepatocytes-like stem cells. Each value was presented as mean \pm standard error of the mean (SEM). **P < 0.01. (d) Cells soft agar colony formation assay. Each value was presented as mean \pm standard error of the mean (SEM). **P < 0.01.

CUDR knockdown decreased the telomere length. However, this action was abrogated in control group. However, both excessive CUDR and CUDR knockdown did significantly alter the telomerase length in hepatocyte-like stem cells without IL6 treatment (Fig. 8d). Intriguingly, our results showed that excessive CUDR increased and CUDR knockdown decreased the microsatellite instability(MSI) in hepatocyte-like stem cells with IL6 treatment (Fig. 8e). Together, CUDR enhances telomerase activity, elongates telomere length and increases microsatellite instability(MSI) in the inflammatory environment through miRs or lncRNAs.

IL6 cooperates with CUDR to aggravate hepatocyte-like stem cells malignant transformation through NF- κ B signaling. To address whether IL6 cooperates with CUDR to aggravate malignant transformation of hepatocyte-like stem cells through NF- κ B signaling, we established hepatocyte-like stem cell lines with CUDR overexpression plus IL6, or CUDR overexpression plus IL6 plus NF- κ B knockdown. As shown in Fig. 9a, CUDR overexpression plus IL6 significantly increased the NF- κ B and Stat3 expression, however, CUDR overexpression plus IL6 plus NF- κ B knockdown significantly decreased the expression of NF- κ B and Stat3 in hepatocyte-like stem cells. As shown in Fig. 9b, excessive CUDR plus IL6 significantly promoted the cell growth

of hepatocyte-like stem cells ($P < 0.01$), however, excessive CUDR combined with IL6 and NF- κ B knockdown did not alter cell growth ability ($P > 0.05$). As shown in Fig. 9c, excessive CUDR plus IL6 significantly increased the BrdU positive rate ($56.72 \pm 8.23\%$ vs $21.317 \pm 4.24\%$, $P < 0.01$) of hepatocyte-like stem cells, however, CUDR overexpression plus IL6 plus NF- κ B knockdown significantly decreased the BrdU positive rate ($13.22 \pm 3.43\%$ vs $21.317 \pm 4.24\%$, $P < 0.01$) ($P < 0.01$). Furthermore, CUDR plus IL6 overexpression significantly increased the colony formation ability ($17.3 \pm 4.67\%$ vs 0, $P < 0.01$) of hepatocyte-like stem cells. However, depletion of NF- κ B fully abrogated the action of CUDR plus IL6 (Fig. 9d). Taken Together, these observations suggest that IL6 cooperates with CUDR to aggravate malignant transformation of hepatocyte-like stem cells through NF- κ B signaling.

Discussion

Long noncoding RNA (lncRNAs) can regulate gene expression in many ways, including chromosome remodeling, transcription and post-transcriptional processing. Moreover, the dysregulation of lncRNAs has increasingly been linked to many human diseases, especially in cancers³⁰. To this data, we revealed that CUDR cooperates with inflammatory cytokine IL6 to triggers the malignant transformation of human embryonic stem cells derived hepatocyte-like stem cells. Mechanistically, our results demonstrate IL6 cooperates with CUDR to promote SUV39h1 expression in the inflammatory environment. Accordingly, the methylation of SUV39h1 mRNA 3' UTR is increased that causes the SUV39h1 mRNA more stable. Furthermore, the excessive SUV39h1 increases three methylation on histone H3 ninth lysine (H3K9me3). Under inflammatory conditions, H3K9me3 promotes the expression and phosphorylation of NF- κ B, in turn, phosphorylated NF- κ B promotes the expression and phosphorylation of Stat3. Importantly, the phosphorylated Stat3 loads onto the promoter region of miR21, miR155, miR17, miR675, miR372, miR192, CUDR, HOTAIR, MALAT1, HULC, H19, as well as excessive CUDR and IL6 increases DNA methylation of MEG3, TERRA promoter region. Therefore, the binding of pStat3 to MEG3, TERRA the promoter regions is decreased that leads to reduce the expression of MEG3, TERRA. Ultimately, the abnormal expression of miRs and lncRNAs results in increased telomerase activity, telomere length and the increased microsatellite instability (MSI), leading to malignant transformation of hepatocyte-like cells eventually (Fig. 10).

Interleukin-6 could induced malignant transformation of stem cells in association with enhanced signaling of Stat3³¹ and myeloid-derived cells endowed stem-like qualities to breast cancer cells through IL6/STAT3 and NO/NOTCH cross-talk signaling³². In particular, IL6 blockade significantly inhibited lung cancer promotion³³. Our results showed that IL6 alone could not prompt malignant transformation of hepatocyte-like stem cells, however, IL6 enhanced the CUDR oncogenic action that triggered malignant transformation of hepatocyte-like stem cells. It suggests IL6 acts as enhancer of tumorigenesis. To our knowledge, this is the first report demonstrating CUDR cooperates with IL6 to trigger malignant transformation of hepatocyte-like cells *in vitro* and *in vivo*.

It is worth mentioning that CUDR plus IL6 may play an important role in the occurrence of hepatocellular carcinoma. In this report, we focused mainly on the view how CUDR plus IL6 functions during hepatocyte-like stem cells' malignant transformation. To this date, accumulating evidence indicates that CUDR was aberrantly upregulated in liver cancer tissues and associated with TNM stage, metastasis and postoperative survival. CUDR depletion inhibited the growth and metastasis of HCC cell lines *in vitro* and *in vivo*. For example, excessive CUDR contributes to progression of hepatocellular carcinoma through inhibition of miR-216b and activation of FGFR1/ERK signaling pathway³⁴. Our present findings are consistent with some reports. Overexpression of the CUDR plus IL6 links a dramatic increase of proliferative and growth capacity. Herein, the involvement of promotion of hepatocyte-like stem cells growth based on CUDR plus IL6 is supported by results from four parallel sets of experiments: 1) excessive CUDR triggers malignant transformation of human embryonic stem cells derived hepatocyte-like stem cells in mouse injury liver inflammation microenvironment; 2) excessive CUDR cooperates with IL6 to aggravate derived hepatocyte-like cells malignant transformation and growth of hepatocyte-like cells *in vitro* and *in vivo*. 3) In IL6 treated groups, excessive CUDR enhanced the mPGES1, TLR4, NF- κ B expression, as well as reduced the 15PGDH expression in these induced hepatocyte-like cells. On the other hand, mPGES1, TLR4, NF- κ B, 15PGDH expression were significantly not changed in IL6 untreated groups. According to the aforementioned findings and reports, it is clear that CUDR plus IL6 has a strong carcinogenic ability.

It has been confirmed that histone H3 lysine 9 trimethylation (H3K9me3) is associated with transcriptional repression and regulated by histone lysine methyltransferases such as suppressor of variegation 3-9 homolog 1 (SUV39H1), a histone methyltransferase. SUV39H1 catalyzes histone 3 lysine 9 trimethylation and is involved in heterochromatin organization and genome stability. Methylation of SUV39H1 facilitated genome instability and ultimately inhibited cell proliferation. SUV39H1 knockdown reduced H3K9me3 levels and impaired HCC cell growth and sphere formation. Elevated SUV39H1 expression and high levels of H3K9me3 have important roles in HCC development and progression^{35,36}. The sustained expression of SUV39H1 delays the repair of constitutive heterochromatin (HC) DNA and reduces clonogenic survival after ionizing irradiation³⁷. Moreover, long H3K9me3-marked domains had lower accessibility, consistent with a more compact chromatin structure³⁸. Dynamic changes in histone modification are critical for regulating DNA double-strand break (DSB) repair, increasing the levels of H3K9me3 in open chromatin domains that lack H3K9me3 and thereby promoting efficient activation of Tip60 and ATM in these regions³⁹. On the other hand, METTL3, an N(6)-methyladenosine (m(6)A) transferase, as a regulator for terminating murine naïve pluripotency. METTL3 knockout preimplantation epiblasts and naïve embryonic stem cells are depleted for m(6)A in mRNAs⁴⁰ and N6-methyladenosine modification destabilizes developmental regulators in embryonic stem cells⁴¹. RNA decoration by m(6)A has a fundamental role in regulation of gene expression⁴². Our data suggest that CUDR enhances SUV39h2 expression and H3K9me3 modification dependent on IL6 on the transcriptional and post-transcriptional mRNA methylation modification level. This assertion is based on several observations in IL6 treated hepatocyte-like stem cells: (1) CUDR facilitated the loading of CREPT (cell-cycle related and expression-elevated protein in tumor) and RNA polymerase II onto SUV39h2 promoter region. (2) CUDR increased the SUV39h2 promoter luciferase

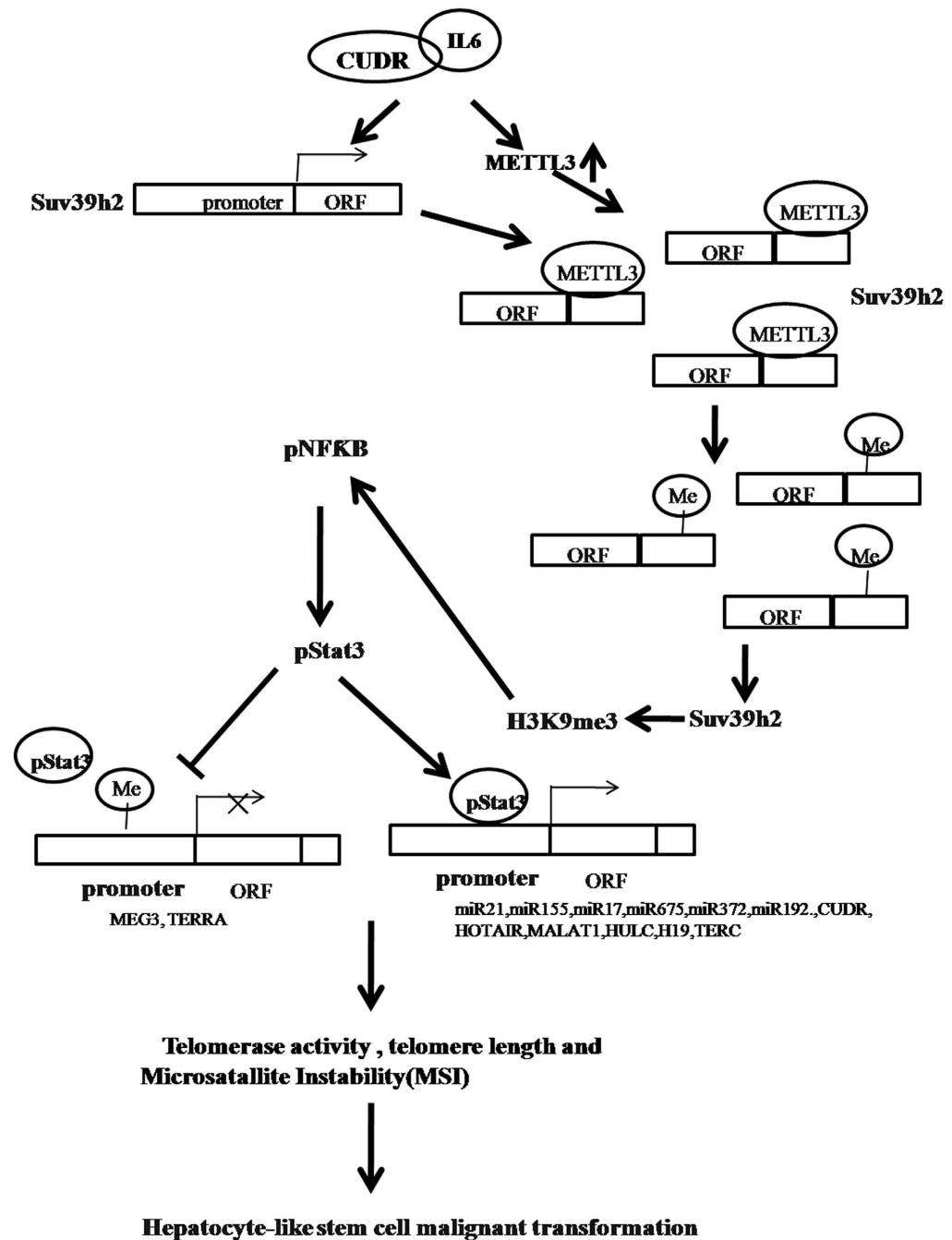


Figure 10. The schematic diagram illustrates a model that IL6 cooperates with CUDR to promote malignant transformation of hepatocyte-like stem cells. The interaction between CUDR and inflammatory cytokine IL6 triggers the malignant transformation of human embryonic stem cells derived hepatocyte-like stem cells. Mechanistically, our results reveal CUDR cooperates with IL6 to promote SUV39h1 high expression at the transcriptional level in the inflammatory environment. Intriguingly, CUDR cooperates with IL6 also to cause METTL3 overexpression that bind to SUV39h1 mRNA. Accordingly, the methylation of SUV39h1 mRNA 3'UTR is increased that causes the SUV39h1 mRNA more stable. Then, the excessive SUV39h1 increases three methylation on histone H3 ninth lysine (H3K9me3). In inflammatory conditions, H3K9me3 promotes the expression and phosphorylation of NF- κ B, and phosphorylated NF- κ B promotes the expression and phosphorylation of Stat3. That phosphorylated Stat3 loads onto the promoter region of miR21, miR155, miR17, miR675, miR372, miR192, CUDR, HOTAIR, MALAT1, HULC, H19 enhances these noncoding RNAs outcome. On the other hand, excessive CUDR and IL6 increases DNA methylation of MEG3, TERRA promoter region. Therefore, the binding of pStat3 to MEG3, TERRA the promoter regions is decreased that leads to reduce the MEG3, TERRA expression. Ultimately, the abnormal expression of miRNAs and lncRNAs results in increased telomerase activity, telomere length and the increased microsatellite instability (MSI), eventually leading to malignant transformation of hepatocyte-like stem cells.

activity. (3) CUDR enhanced the METTL3 expression. (4) CUDR enhanced the binding of METTL3 to SUV39h2 mRNA; (5) CUDR enhanced the mRNA methylation of SUV39h2; (6) CUDR enhanced SUV39h2 mRNA expression; (7) CUDR enhanced SUV39h2 expression, phosphorylation and sumoylation. (8) CUDR enhanced three methylation on histone H3 ninth lysine (H3K9me3).

Sumoylation belongs to the host cell posttranslational modification system which is an enzymatic process that is biochemically analogous to, but functionally distinct from, ubiquitinylation. Conjugation of SUMO does not typically lead to degradation of the substrate. It is clear that this modification system is an important regulator of intracellular protein localization, particularly involving nuclear uptake and punctate intranuclear accumulation^{43,44}. In the report, our findings showed that CUDR enhanced SUV39h2 expression through sumoylation.

FTO gene encodes an N(6)-methyladenosine (m(6)A) RNA demethylase. The most abundant mRNA post-transcriptional modification is N(6)-methyladenosine (m(6)A), which has broad roles in RNA biology by limiting the m(6)A 'eraser' FTO from demethylation^{45,46}. However, CUDR overexpression or knockdown did not alter the FTO expression in IL6 treated hepatocyte-like cells. It suggests CUDR combined with IL6 could enhance RNA methylase activity, however, did not alter RNA demethylase in hepatocyte-like cells.

NF κ B has been associated with a number of inflammatory diseases while persistent inhibition of NF κ B leads to inappropriate immune cell development or delayed cell growth^{47,48}. To this data, Our observations suggest that CUDR plus IL6 enhances expression and phosphorylation of NF- κ B through SUV39h2 under the inflammatory condition. This assertion is based on several observations: 1) CUDR promoted the interplay between SUV39h2 and HistoneH3. Therefore, excessive CUDR promoted the modifications of mono-, double-, tri-methylation on the ninth lysine of Histone H 3 (H3K9me1, H3K9me2, H3K9me3); 2) CUDR promoted NF κ B promoter-enhancer looping formation and the H3K9me3, RNA polymerase II entering into the loop in these hepatocyte-like cells treated with IL6; 3) CUDR promoted NF κ B promoter luciferase activity in these hepatocyte-like cells treated with IL6. 4) excessive CUDR promoted expression and its phosphorylation of NF κ B in these hepatocyte-like stem cells treated with IL6. Inaword, these findings are noteworthy that CUDR plus IL6 links to cancer cells growth in the inflammatory environment.

It is worth noting that Stat3 activity alteration is absorbing and of great concern. STATs can be activated independently of JAKs, most notably by c-Src kinases. Several approaches have been used to inhibit STAT3 in the hope of developing an antitumor agent^{49,50}. Strikingly, STAT3 regulates the migration and invasion of a stem-like subpopulation through microRNA-21 and multiple targets in hepatocellular carcinoma⁵¹. We observed that excessive CUDR cooperates with IL6 to enhance expression and phosphorylation of Stat3 dependent on NF- κ B phosphorylation. It is evident that activation of Stat3 may play an important role in hepatocyte-like cells malignant transformation. Our findings in this study provide novel evidence for an active role of Stat3 promotion of liver cancer stem cell growth. This assertion is based on several observations: 1) CUDR enhanced the pNF κ B occupancy on the Stat3 promoter region. 2) CUDR increased the Stat3 promoter luciferase activity in hepatocyte-like cells treated with IL6. 3) CUDR promotes the Stat3 transcription, translation and its phosphorylation in hepatocyte-like cells without treated with IL6.

Strikingly, our results show CUDR plus IL6 alters microRNAs and lncRNAs expression through pStat3 in hepatocyte-like cells. Herein, our findings show that CUDR alters microRNAs and lncRNAs expression through pStat3 in the inflammatory environment dependent on IL6. The conclusion is supported by results from nine parallel sets of experiments: 1) CUDR enhanced the loading of pStat3 on the promoter region of miR21, miR155, miR17, miR675, miR372, miR192. 2) CUDR overexpression increased the miR21, miR155, miR17, miR675, miR372, miR192 promoter luciferase activity. 3) CUDR overexpression enhanced the expression of miR21, miR155, miR17, miR675, miR372, miR192; 4) CUDR enhanced the loading of pStat3 on the promoter region of CUDR, HOTAIR, MALAT1, HULC, H19. 5) CUDR inhibited the loading of pStat3 on the promoter region of MEG3, TERRA; 6) CUDR increased the TERRA and MEG3 methylation on promoter region. 7) CUDR decreased the TERRA promoter luciferase activity; 8) CUDR promoted the expression CUDR, HOTAIR, MALAT1, HULC, H19, as well as CUDR inhibited the expression MEG3 and TERRA; 9) CUDR promoted the expression HOTAIR, MALAT1, HULC H19, as well as CUDR inhibited the expression MEG3 and TERRA.

It is well known that DNA mismatch repair (MMR) ensures replication fidelity by correcting mismatches generated during DNA replication⁵². Proper telomeric chromatin configuration is thought to be essential for telomere homeostasis and stability⁵³. The human telomerase reverse transcriptase catalytic subunit (TERT) contributes to cell physiology independently of its ability to elongate telomeres⁵⁴. Telomeres have been considered to be silent, but it was recently demonstrated that mammalian telomeres are transcribed into telomeric repeat-containing RNA (TERRA). TERRA participates in the regulation of telomere length, telomerase activity and heterochromatinization⁵⁵. Our results showed that CUDR cooperated with IL6 to enhance telomerase activity, elongate telomere length and increase Microsatellite Instability(MSI). This assertion is based on several observations: in IL6 treated hepatocyte-like stem cells, 1) CUDR increased the interplay between TERT and TERC, as well as CUDR overexpression inhibited the interaction between TERT and TERRA; 2) excessive CUDR increased the telomerase activity in IL6 treated hepatocyte-like cells; 3) excessive CUDR increased the telomere length; 4) excessive CUDR increased the telomere length; 5) excessive CUDR increased the Microsatellite Instability(MSI) in IL6 treated hepatocyte-like cells.

Many questions remained about the function of CUDR combined with inflammatory factor. For example, what causes strong oncogenic action CUDR plus IL6 inflammatory factor? How does CUDR cooperates with inflammatory factor? Does CUDR enhance malignant differentiation of liver stem cells? Does CUDR regulate a series of molecular events during malignant differentiation of liver stem cells? Answering these questions will help understand the mechanism about malignant differentiation of liver stem cell. **In summary**, our present data indicated that CUDR combined with inflammatory factor promotes malignant progression of liver stem cells through epigenetic hallmark. These observations provide insight into a novel link between CUDR and

inflammatory cytokines during hepatocarcinogenesis. To understand the novel functions of CUDR will help in the development of new liver cancer therapeutic and diagnostic approaches.

Experimental Procedures

Ethics statement. All methods were carried out in “accordance” with the approved guidelines. All experimental protocols “were approved by” a Tongji university institutional committee. Informed consent was obtained from all subjects. The study was reviewed and approved by the China national institutional animal care and use committee”.

Cell Lines. Human embryonic stem (ES) cells line MEL-2 (Merck Millipore, Darmstadt, Germany) were maintained in HEScGRO Medium (1000IU/ml LIF) (Merck Millipore, Darmstadt, Germany) supplemented with 10% heat-inactivated fetal bovine serum (Gibco BRL Life Technologies, Grand Island, NY) on matrigel (0.1% gelatin solution or human collagen IV coating material) in a humidified atmosphere of 5% CO₂ incubator at 37 °C.

Intravenous transplantation of the hepatocyte-like stem cells. Viable hepatoblasts (10⁸ cells/mouse) were inoculated i.v. into Balb/C mice. The Balb/C mice were observed over 8 weeks for tumor formation. Animals were stratified so that the mean tumor sizes in all groups were nearly identical. The mice were then sacrificed and the tumors recovered.

Cell transfection and stable cell lines. Cells were transfected with DNA plasmids using transfast transfection reagent lipofectamine^R 2000 (Invitrogen) according to manufacturer’s instructions.

RT-PCR. Total RNA was purified using Trizol (Invitrogen) according to manufacturer’s instructions. cDNA was prepared by using oligonucleotide (dT)_{17–18}, random primers, and a SuperScript First-Strand Synthesis System (Invitrogen). PCR analysis was performed under the special conditions. β-actin was used as an internal control.

Co-immunoprecipitation (IP). Cells were lysed in 1 ml of the whole-cell extract buffer A (50 mM pH7.6 Tris-HCl, 150 mM NaCl, 1%NP40, 0.1 mM EDTA, 1.0 mM DTT, 0.2 mM PMSF, 0.1 mM Pepstatine, 0.1 mM Leupeptine, 0.1 mM Aprotine). Five-hundred-microliter cell lysates was used in immunoprecipitation with antibody. In brief, protein was pre-cleared with 30 μl protein G/A-plus agarose beads (Santa Cruz, Biotechnology, Inc. CA) for 1 hour at 4 °C and the supernatant was obtained after centrifugation (5,000 rpm) at 4 °C. Pre-cleared homogenates (supernatant) were incubated with 2 μg of antibody and/or normal mouse/rabbit IgG by rotation for 4 hours at 4 °C, and then the immunoprecipitates were incubated with 30 μl protein G/A-plus agarose beads by rotation overnight at 4 °C, and then centrifuged at 5000 rpm for 5 min at 4 °C. The precipitates were washed five times × 10 min with beads wash solution (50 mM pH7.6 TrisCl, 150 mM NaCl, 0.1%NP-40, 1 mM EDTA) and then resuspended in 60 μl 2 × SDS-PAGE sample loading buffer to incubate for 5–10 min at 100 °C. Then Western blot was performed with a another related antibody indicated in Western blotting.

Chromatin immunoprecipitation (CHIP). Cells were cross-linked with 1% (v/v) formaldehyde (Sigma) for 10 min at room temperature and stopped with 125 mM glycine for 5 min. Crossed-linked cells were washed with phosphate-buffered saline, resuspended in lysis buffer, and sonicated for 8–10 min in a SONICS VibraCell to generate DNA fragments with an average size of 500 bp or so. Chromatin extracts were diluted 5-fold with dilution buffer, pre-cleared with Protein-A/G-Sepharose beads, and immunoprecipitated with specific antibody on Protein-A/G-Sepharose beads. After washing, elution and de-cross-linking, the ChIP DNA was detected by either traditional PCR.

Chromosome conformation capture (3C)-CHIP. Antibody-specific immunoprecipitated chromatin was obtained as described above for ChIP assays. PCR products were run on a 2% agarose gel. Each validation experiment was repeated at least twice.

Methylation analysis. Methylated DNA Immunoprecipitation (MeDIP)-Dot blot-western blotting with anti-5-Methylcytosine (5-mC) and ethylation analysis by MspI plus BamHI digestion.

Soft agar colony formation assay. 2 × 10² cells were plated on a 6 well plate containing 0.5% (lower) and 0.35% (upper) double layer soft-agar. The cells in six well plates were incubated at 37 °C in humidified incubator for 21 days. The cells were fed 1–2 times per week with cell culture media (DMEM). Soft-agar colonies on the 6 well plates were stained with 0.5 ml of 0.05% Crystal Violet for more than 1 hour and the colonies were counted.

Statistical analysis. The significant differences between mean values obtained from at least three independent experiments. Each value was presented as mean ± standard error of the mean (SEM) unless otherwise noted, with a minimum of three replicates. Student’s t-test was used for comparisons, with P < 0.05 considered significant.

References

1. Borhani-Haghighi, M., Talaie-Khozani, T., Ayatollahi, M. & Vojdani, Z. Wharton’s Jelly-derived Mesenchymal Stem Cells can Differentiate into Hepatocyte-like Cells by HepG2 Cell Line Extract. *Iran J Med Sci.* **40**(2), 143–151 (2015).
2. Kamiya, A. & Chikada, H. Human pluripotent stem cell-derived cholangiocytes: current status and future applications. *Curr Opin Gastroenterol.* **31**(3), 233–238 (2015).
3. Ishikawa, T. *et al.* Human induced hepatic lineage-oriented stem cells: autonomous specification of human iPSC cells toward hepatocyte-like cells without any exogenous differentiation factors. *PLoS One.* **10**(4), e0123193 (2015).

4. Dubois-Pot-Schneider, H. *et al.* Inflammatory cytokines promote the retrodifferentiation of tumor-derived hepatocyte-like cells to progenitor cells. *Hepatology*. **60**(6), 2077–2090 (2014).
5. Jung, I. H. *et al.* Predominant Activation of JAK/STAT3 Pathway by Interleukin-6 Is Implicated in Hepatocarcinogenesis. *Neoplasia*. **17**(7), 586–597 (2015).
6. Zhang, Q. *et al.* Tet2 is required to resolve inflammation by recruiting Hdac2 to specifically repress IL-6. *Nature*. **525**(7569), 389–393 (2015).
7. Haiyan, Li *et al.* LncRNA HOTAIR promotes human liver cancer stem cell malignant growth through downregulation of SETD2. *Oncotarget* **6**(29), 27847–27864 (2015).
8. Haiyan Li *et al.* miR675 upregulates long noncoding RNA H19 through activating EGR1 in human liver cancer. *Oncotarget* **6**(31), 31958–31984 (2015).
9. Han, Y. *et al.* UCA1, a long non-coding RNA up-regulated in colorectal cancer influences cell proliferation, apoptosis and cell cycle distribution. *Pathology*. **46**(5), 396–401 (2015).
10. Li, Z., Li, X., Wu, S., Xue, M. & Chen, W. LncRNA-UCA1 Promotes Glycolysis by Upregulating Hexokinase 2 through mTOR-STAT3/miR143 Pathway. *Cancer Sci*. **105**(8), 951–955 (2014).
11. Xue, M., Li, X., Li, Z. & Chen, W. Urothelial carcinoma associated 1 is a hypoxia-inducible factor-1 α -targeted long noncoding RNA that enhances hypoxic bladder cancer cell proliferation, migration, and invasion. *Tumour Biol*. **35**(7), 6901–6912 (2014).
12. Kumar, P. P. *et al.* Coordinated control of senescence by lncRNA and a novel T-box3 co-repressor complex. *Elife*. e02805 (2014).
13. Jiang, M. *et al.* A novel long non-coding RNA-ARA: adriamycin resistance-associated. *Biochem Pharmacol*. **87**(2), 254–283 (2015).
14. Wu, W. *et al.* Ets-2 regulates cell apoptosis via the Akt pathway, through the regulation of urothelial cancer associated 1, a long non-coding RNA, in bladder cancer cells. *PLoS One*. **8**(9), e73920 (2013).
15. Kaneko, K. *et al.* Gene expression profiling reveals upregulated UCA1 and BMF in gallbladder epithelia of children with pancreaticobiliary maljunction. *J Pediatr Gastroenterol Nutr*. **52**(6), 744–750 (2011).
16. Wang, X. S. *et al.* Rapid identification of UCA1 as a very sensitive and specific unique marker for human bladder carcinoma. *Clin Cancer Res*. **12**(16), 4851–4858 (2006).
17. Li, J. Y. & Ma, X., Zhang CB. Overexpression of long non-coding RNA UCA1 predicts a poor prognosis in patients with esophageal squamous cell carcinoma. *Int J Clin Exp Pathol*. **7**(11), 7938–7944 (2014).
18. Xin, Gui, Haiyan, Li, Tianming, Li, Hu, Pu & Dongdong, Lu. Long noncoding RNA CUDR regulates HULC and β -Catenin to govern human liver stem cell malignant differentiation. *Molecular Therapy*. **23**(12), 1843–1853 (2015).
19. Hu Pu *et al.* CUDR promotes liver cancer stem cell growth through upregulating TERT and C-Myc. *Oncotarget* **6**(38), 40775–40798 (2015).
20. Wang, X. *et al.* N6-methyladenosine-dependent regulation of messenger RNA stability. *Nature*. **505**(7481), 117–120 (2014).
21. Alarcón, C. R., Lee, H., Goodarzi, H., Halberg, N. & Tavazoie, S. F. N6-methyladenosine marks primary microRNAs for processing. *Nature*. **519**(7544), 482–485 (2015).
22. Geula, S. *et al.* Stem cells. m6A mRNA methylation facilitates resolution of naïve pluripotency toward differentiation. *Science*. **347**(6225), 1002–1006 (2015).
23. Kravtsova-Ivantsiv, Y. *et al.* KPC1-mediated ubiquitination and proteasomal processing of NF- κ B1 p105 to p50 restricts tumor growth. *Cell*. **161**(2), 333–347 (2015).
24. Saha, S. *et al.* Sulphur alters NF κ B-p300 cross-talk in favour of p53-p300 to induce apoptosis in non-small cell lung carcinoma. *Int J Oncol*. **47**(2), 573–582 (2015).
25. An, X. L. *et al.* Metformin suppresses pancreatic tumor growth with inhibition of NF κ B/STAT3 inflammatory signaling. *Pancreas*. **44**(4), 636–647 (2015).
26. Véquaud, E. *et al.* YM155 potently triggers cell death in breast cancer cells through an autophagy-NF- κ B network. *Oncotarget*. **6**(15), 13476–13486 (2015).
27. Wang, T. *et al.* Anxa2 binds to STAT3 and promotes epithelial to mesenchymal transition in breast cancer cells. *Oncotarget*. **6**(31), 30975–30992 (2015).
28. Yoshioka, H., Nonogaki, T., Fukuishi, N. & Onosaka, S. Calcium-deficient diet attenuates carbon tetrachloride-induced hepatotoxicity in mice through suppression of lipid peroxidation and inflammatory response. *Heliyon*. **2**(6), e00126 (2016).
29. Heimberg, M., Watkins, M. L. & Tooker, R. Carbon tetrachloride (CCL4) hepatotoxicity: the direct action of CCL4 on the liver. *J Pharmacol Exp Ther*. **145**, 92–101 (1964).
30. H., Shi X., Sun M., Liu H., Yao Y., Song & Y. Long non-coding RNAs: a new frontier in the study of human diseases. *Cancer Lett*. **339**(2), 159–166 (2013).
31. Cui, X., Liu, J., Bai, L., Tian, J. & Zhu, J. Interleukin-6 induces malignant transformation of rat mesenchymal stem cells in association with enhanced signaling of signal transducer and activator of transcription 3. *Cancer Sci*. **105**(1), 64–71 (2014).
32. Peng, D., *et al.* Myeloid-derived suppressor cells endow stem-like qualities to breast cancer cells through IL6/STAT3 and NO/NOTCH cross-talk signaling. *Cancer Res*. **76**(11), 3156–3165 (2016).
33. Caetano, M. S., Zhang, H., Cumpian, A. M., Gong, L., Unver, N., Ostrin, E. J., Daliri, S., Chang, S. H., Ochoa, C. E., Hanash, S., Behrens, C., Wistuba, I. I., Sternberg, C., Kadara, H., Ferreira, C. G., Watowich S. S. & Moghaddam, S. J. IL6 blockade reprogramsthe lung tumor microenvironment to limit the development and progression of K-ras-mutant lung cancer. *Cancer Res*. **76**(11), 3189–3199 (2016).
34. Wang F. *et al.* Upregulated lncRNA-UCA1 contributes to progression of hepatocellular carcinoma through inhibition of miR-216b and activation of FGFR1/ERK signaling pathway. *Oncotarget*. **6**(10), 7899–7917 (2015).
35. Chiba, T. *et al.* Histone lysine methyltransferase SUV39H1 is a potent target for epigenetic therapy of hepatocellular carcinoma. *Int J Cancer*. **36**(2), 89–89 (2015).
36. Zheng H., Chen, L., Pledger, W. J., Fang, J. & Chen, J. p53 promotes repair of heterochromatin DNA by regulating JMJD2b and SUV39H1 expression. *Oncogene*. **33**(6), 34–44 (2014).
37. Geula, S. *et al.* m6A mRNA methylation facilitates resolution of naïve pluripotency toward differentiation. *Science*. **347**(6225), 002–006 (2015).
38. Alarcón, C. R., Lee, H., Goodarzi, H., Halberg, N. & Tavazoie S. F. N6-methyladenosine marks primary microRNAs for processing. *Nature*. **519**(7544), 82–85 (2015).
39. Wang, Y. *et al.* N6-methyladenosine modification destabilizes developmental regulators in embryonic stem cells. *Nat Cell Biol*. **16**(2), 91–98 (2014).
40. Lay F. D. *et al.* The role of DNA methylation in directing the functional organization of the cancer epigenome. *Genome Res*. **25**(4), 67–77 (2015).
41. Chen, B. *et al.* Mdig de-represses H19 large intergenic non-coding RNA (lincRNA) by down-regulating H3K9me3 and heterochromatin. *Oncotarget*. **4**(9), 427–437 (2013).
42. Abu-Remaileh, M. *et al.* Chronic inflammation induces a novel epigenetic program that is conserved in intestinal adenomas and in colorectal cancer. *Cancer Res*. **75**(10), 120–130 (2015).
43. Wilson, V. G. & Rangasamy, D. Intracellular targeting of proteins by sumoylation. *Exp Cell Res*. **271**(1), 57–65 (2001).
44. Ding, X., Wang, A., Ma, X., Demarque M., Jin, W., Xin, H., Dejean, A. & Dong, C. Protein SUMOylation is required for regulatory T cell expansion and function. *Cell Rep*. **16**(4), 1055–1066 (2016).

45. Zhou, J. *et al.* Dynamic m(6)A mRNA methylation directs translational control of heat shock response. *Nature*. **526(7574)**, 591–594 (2015)
46. Ben-Haim, M. S., Moshitch-Moshkovitz, S. & Rechavi, G. FTO: linking m6A demethylation to adipogenesis. *Cell Res*. **25(1)**, 3–4 (2015).
47. Zha, X. *et al.* NF κ B up-regulation of glucose transporter 3 is essential for hyperactive mammalian target of rapamycin-induced aerobic glycolysis and tumor growth. *Cancer Lett.* **359(1)**, 97–106 (2015).
48. Ishise H. *et al.* Hypertrophic scar contracture is mediated by the TRPC3 mechanical force transducer via NF κ B activation. *Sci. Rep.* **5**, 11620, doi:10.1038/srep11620 (2015).
49. Giunti, L. *et al.* Anti-miR21 oligonucleotide enhances chemosensitivity of T98G cell line to doxorubicin by inducing apoptosis. *Am J Cancer Res.* **5(1)**, 231–242 (2014).
50. Li, H., Rokavec, M. & Hermeking, H. Soluble IL6R represents a miR-34a target: potential implications for the recently identified IL-6R/STAT3/miR-34a feed-back loop. *Oncotarget*. **6(16)**, 14026–14032 (2015).
51. Zhang, N. *et al.* STAT3 regulates the migration and invasion of a stem-like subpopulation through microRNA-21 and multiple targets in hepatocellular carcinoma. *Oncol Rep.* **33(3)**, 1493–1498 (2013).
52. Thompson, B. A. & Spurdle, A. B. Microsatellite instability use in mismatch repair gene sequence variant classification. *Genes (Basel)*. **6(2)**, 150–162 (2015).
53. Maida, Y. *et al.* An RNA-dependent RNA polymerase formed by TERT and the RMRP RNA. *Nature*. **461(7261)**, 230–235 (2009).
54. Ting, N. S., Pohorelic, B., Yu, Y., Lees-Miller, S. P. & Beattie, T. L. The human telomerase RNA component, hTR, activates the DNA-dependent protein kinase to phosphorylate heterogeneous nuclear ribonucleoprotein A1. *Nucleic Acids Res.* **37(18)**, 105–115 (2009).
55. Wang, C., Zhao, L. & Lu, S. Role of TERRA in the regulation of telomere length. *nt J Biol Sci.* **11(3)**, 316–323 (2015).

Acknowledgements

This study was supported by grants from National Natural Science Foundation of China (NCSF No. 81272291), National Natural Science Foundation of China (NCSF No. 81572773), Science and Technology Commission of Shanghai Municipality (No. 13JC1405500-13JC1405501).

Author Contributions

Dongdong Lu conceived the study and participated in the study design, performance, coordination and manuscript writing. Qidi Zheng, Zhuojia Lin, Xiaonan Li, Xiaoru Xin, Mengying Wu, Jiahui An, Xin Gui, Tianming Li, Hu Pu, Haiyan Li performed the research. All authors have read and approved the final manuscript.

Additional Information

Supplementary information accompanies this paper at <http://www.nature.com/srep>

Competing financial interests: The authors declare no competing financial interests.

How to cite this article: Zheng, Q. *et al.* Inflammatory cytokine IL6 cooperates with CUDR to aggravate hepatocyte-like stem cells malignant transformation through NF- κ B signaling. *Sci. Rep.* **6**, 36843; doi: 10.1038/srep36843 (2016).

Publisher's note: Springer Nature remains neutral with regard to jurisdictional claims in published maps and institutional affiliations.



This work is licensed under a Creative Commons Attribution 4.0 International License. The images or other third party material in this article are included in the article's Creative Commons license, unless indicated otherwise in the credit line; if the material is not included under the Creative Commons license, users will need to obtain permission from the license holder to reproduce the material. To view a copy of this license, visit <http://creativecommons.org/licenses/by/4.0/>

© The Author(s) 2016

supplementary information

Inflammatory cytokine IL6 cooperates with CUDR to aggravate hepatocyte-like stem cells malignant transformation through NF- κ B signaling

Qidi Zheng¹, Zhuojia Lin¹, Xiaonan Li¹, Xiaoru Xin¹,
Mengying Wu¹,
Jiahui An¹,
Xin Gui¹,
Tianming Li¹,
Hu Pu¹,
Haiyan Li¹,
Dongdong Lu^{1,*}

¹School of Life Science and Technology, Tongji University , Shanghai(200092),
China

* Corresponding author: *Dongdong Lu*, Tongji University School of Life Science and
Technology, Shanghai(200092), China. E-mail: ludongdong@tongji.edu.cn

supplementary Experimental Procedures

Ethics statement All methods were carried out in "accordance" with the approved guidelines. All experimental protocols "were approved by" a Tongji university institutional committee. Informed consent was obtained from all subjects. The study was reviewed and approved by the China national institutional animal care and use committee".

Cell Lines and Plasmids Human embryonic stem (ES) cells line MEL-2(Merck Millipore, Darmstadt, Germany) were maintained in HEScGRO Medium(1000IU/ml LIF)(Merck Millipore, Darmstadt, Germany) supplemented with 10% heat-inactivated fetal bovine serum (Gibco BRL Life Technologies ,Grand Island,NY) on matrigel (0.1 % gelatin solution or human collagen IV coating material) in a humidified atmosphere of 5% CO₂ incubator at 37°C. Mitotically inactivated HS27 feeder cells (ATCC,Manassas,VA) plated at 80,000 cells/cm². Plasmid pGFP-V-RS, pCMV6-A-GFP were purchased from Origene (Rockville, MD 20850,USA).pGL3-NFκB promoter, pGL3-Stat3 promoter were purchased from Addgene(Cambridge MA,USA).pGL3-miR21 promoter, pGL3-miR155 promoter , pGL3-miR17 promoter , pGL3-miR675 promoter, pGL3-miR372 promoter , pGL3-miR192 promoter CUDR, pGL3-HOTAIR promoter, pGL3-MALAT1-promoter, pGL3-MEG3 promoter , pGL3-HULC promoter, pGL3-H19 promoter, pGL3-TERRA promoter, pGL3-TERC promoter pGFP-V-RS-CUDR, pCMV6-A-CUDR were constructed by ourselves.

Embryonic stem (ES) cells differentiate into hepatocyte-like cell in vitro Human ES cell line MEL-2 could efficiently generate definitive endoderm (DE) tissue by treating the modified cultures with high concentrations of the TGFβ family ligand activin A(100 ng/ml, R&D, Minneapolis) for 5 days. A number of groups have generated hepatoblasts using this DE tissue as a starting material, plating the DE on matrix (e.g. collagen) to mimic the hepatic ECM and then added FGF4(100 ng/ml,R&D) and BMP(100 ng/ml ,R&D, Minneapolis) to mimic hepatic induction for 6 days (induced hepatoblasts). This is followed by some combination of insulin, transferrin, selenite(ITS,5μg/ml, R&D, Minneapolis), HGF(20ng/ml, R&D, Minneapolis),OSM(10ng/ml, R&D, Minneapolis),aFGF(50ng/ml, R&D, Minneapolis)

and Dexamethasone(10^{-7} M, R&D, Minneapolis) to expand the hepatoblasts population and to promote hepatic maturation for 10 days.

Mouse Liver *In Vivo* Transfection Systemic administration (i.v. Final injection volume 0.5ml) of Balb/C mouse (20-24g) using Liver *In Vivo* Transfection Reagent (Altogen Biosystems, Las Vegas, NV 89107,USA) conjugated with plasmid DNA. In brief, first, dilute 60 μ g of plasmid DNA in 100 μ l RNase-/DNase-free water vortex gently. Secondly, add 100 μ l of diluted DNA to the sterile tube containing 50 μ l Transfection Reagent and incubate for 15-20 minutes at room temperature. Thirdly, add 10 μ l of Transfection Enhancer Reagent vortex gently and incubate for 5 minutes at room temperature. Then add required amount of sterile solution of 5% glucose (w/v) for injecting animals. The delivery efficiency can be significantly increased by performing repeat injection at least 12 hours after first injection till stable intergration. The use of mice for this work was reviewed and approved by the institutional animal care and use committee in accordance with China national institutes of health guidelines.

RT-PCR Total RNA was purified using Trizol (Invitrogen) according to manufacturer's instructions. cDNA was prepared by using oligonucleotide (dT)₁₇₋₁₈, random primers, and a SuperScript First-Strand Synthesis System (Invitrogen). PCR analysis was performed under the special conditions. β -actin was used as an internal control.

Western Blotting The logarithmically growing cells were washed twice with ice-cold phosphate-buffered saline (PBS, Hyclone) and lysed in a RIPA lysis buffer. Cells lysates were centrifuged at 12,000g for 20 minutes at 4°C after sonication on ice, and the supernatant were separated. After being boiled for 5-10 minutes in the presence of 2-mercaptoethanol, samples containing cells proteins were separated on a 10% sodium dodecyl sulfate-polyacrylamide gel electrophoresis (SDS-PAGE) and transferred onto a nitrocellulose membranes (Invitrogen, Carlsbad, CA,USA). Then blocked in 10% dry milk-TBST (20mM Tris-HCl [PH 7.6], 127mM NaCl, 0.1% Tween 20) for 1 h at 37°C. Following three washes in Tris-HCl pH 7.5 with 0.1% Tween 20, the blots were incubated with 0.2 μ g/ml of antibody(appropriate dilution)

overnight at 4°C. Following three washes, membranes were then incubated with secondary antibody for 60 min at 37°C or 4°C overnight in TBST. Signals were visualized by ECL.

Co-immunoprecipitation(IP) Cells were lysed in 1 ml of the whole-cell extract buffer A(50mM pH7.6 Tris-HCl, 150mM NaCl, 1%NP40, 0.1mMEDTA,1.0mM DTT,0.2mMPMSF, 0.1mM Pepstatine,0.1mM Leupeptine,0.1mM Aproine). Five-hundred-microliter cell lysates was used in immunoprecipitation with antibody. In brief, protein was pre-cleared with 30µl protein G/A-plus agarose beads (Santa Cruz, Biotechnology,Inc.CA) for 1 hour at 4°C and the supernatant was obtained after centrifugation (5,000rpm) at 4°C. Precleared homogenates(supernatant) were incubated with 2 µg of antibody and/or normal mouse/rabbit IgG by rotation for 4 hours at 4°C,and then the immunoprecipitates were incubated with 30µl protein G/A-plus agarose beads by rotation overnight at 4°C,and then centrifuged at 5000rpm for 5 min at 4°C. The precipitates were washed five times×10min with beads wash solution(50 mM pH7.6 TrisCl,150mMNaCl,0.1%NP-40,1mM EDTA) and then resuspended in 60µl 2×SDS-PAGE sample loading buffer to incubate for 5-10 min at 100°C. Then Western blot was performed with a another related antibody indicated in Western blotting.

RNA Immunoprecipitation(RIP) Cells were lysed (15 min, 0°C) in 100 mM KCl, 5 mM MgCl₂, 10 mM HEPES [pH 7.0], 0.5% NP40, 1 mM DTT, 100 units/ml RNase OUT (Invitrogen), 400 µM vanadyl-ribonucleoside complex and protease inhibitors (Roche), clarified and stored on at -80°C. Ribonucleoprotein particle-enriched lysates were incubated with protein A/G-plus agarose beads (Santa Cruz, Biotechnology, Inc.CA) together with antibody or normal mouse or rabbit IgG for 4 hours at 4°C. Beads were subsequently washed four times with 50 mM Tris-HCl(pH 7.0), 150 mM NaCl, 1 mM MgCl₂, and 0.05% NP-40, and twice after addition of 1M Urea. Immunoprecipitates(IPs) were digested with proteinase K (55°C; 30') and mRNAs were then isolated and purified. RT-PCR was performed with the primers as follows: CUDR/P1:5'-atgagtcctcatctctcca-3'; CUDR/P2: 5'-taatgtaggtggcgatgagt-3'.

Chromatin immunoprecipitation (CHIP) assay Cells were cross-linked with 1% (v/v) formaldehyde (Sigma) for 10 min at room temperature and stopped with 125 mM glycine for 5 min. Crossed-linked cells were washed with phosphate-buffered saline, resuspended in lysis buffer, and sonicated for 8-10 min in a SONICS VibraCell to generate DNA fragments with an average size of 500 bp or so. Chromatin extracts were diluted 5-fold with dilution buffer, pre-cleared with Protein-A/G-Sepharose beads, and immunoprecipitated with specific antibody on Protein-A/G-Sepharose beads. After washing, elution and de-cross-linking, the ChIP DNA was detected by either traditional PCR.

Chromosome conformation capture (3C) –chromatin immunoprecipitation (ChIP) assay (ChIP-3C/ChIP-Loop assays) Antibody-specific immunoprecipitated chromatin was obtained as described above for ChIP assays. Chromatin still bound to the antibody-Protein-A/G-Sepharose beads were resuspended in 500 μ l of 1.2 \times restriction enzyme buffer at 37 °C for 1 h. 7.5 μ l of 20% SDS was added, the mixture was incubated for 1 h, followed by addition of 50 μ l of 20% Triton X-100, and then incubation for an additional 1 h. Samples were then incubated with 400 units of selected restriction enzyme at 37 °C overnight. After digestion, 40 μ l of 20% SDS was added to the digested Chromatin, and the mixture was incubated at 65 °C for 10 min. 6.125 ml of 1.15 \times ligation buffer and 375 μ l of 20% Triton X-100 was added, the mixture was incubated at 37 °C for 1 h, and then 2000 units of T4 DNA ligase was added at 16 °C for a 4-h incubation. Samples were then de-cross-linked at 65 °C overnight followed by phenol-chloroform extraction and ethanol precipitation. After purification, the ChIP-3C material was detected for long range interaction with specific primers. All primers had to be within a region of \pm 150 bp from the restriction enzyme digestion site. PCR products were amplified with AccuPrime Tag High Fidelity DNA Polymerase (Invitrogen) for 35 cycles. PCR products were run on a 2% agarose gel. Each validation experiment was repeated at least twice.

Dual Luciferase Reporter Assay Cells (1×10^5 /well of a six-well plate) were transiently transfected with 1 μ g of luciferase construct and 0.1 μ g of pRL-tk (promega) or indicated plasmids with the use of the Lipofectamine™ 2000

(Invitrogen) . After incubation for 24 h, the cells were harvested with Passive Lysis Buffer (Promega), and luciferase activities of cell extracts were measured with the use of the Dual luciferase assay system (Promega) according to manufacturer's instructions. luciferase activity was measured and normalized for transfection efficiency with Renilla luciferase activity. Transfection was performed with at least three different batches of each reporter plasmid.

Nuclear Run on assay Nuclear run-on was performed by supplying biotin-probe to nuclei, and labeled transcripts were bound to streptavidin-coated streptavidin-agarose Resin. The cells are chilled, and the membranes are permeabilized or lysed. The nuclei are then incubated for a short time at 37 °C in the presence of nucleoside triphosphates (NTPs) and biotin labeled probe. The number of nascent transcripts on the gene at the time of chilling is thought to be proportional to the frequency of transcription initiation. To determine the relative number of nascent transcripts in each sample, the biotin labeled RNA is purified and hybridized to a membrane containing immobilized DNA from the gene of interest. The amount of biotin activity that hybridizes to the membrane is approximately proportional to the number of nascent transcripts.

MSI detection through Dot blot (Slot blot) Dot blots can only confirm the presence or absence of a biomolecule or biomolecules which can be detected by the DNA probes. Various Biotin labling MSI probes (Biotin-MSIs) added individually to the wells where a vacuum sucks the water (with NaOH and NH₄OAc) from underneath the membrane (nitrocellulose) as a dot and then is spotted through circular templates directly. The cells DNA is quantified and equal amounts are aliquoted into tubes. These are denatured (NaOH and 95° C) and can be hybridized with the membrane to allow for the detection of variation between samples. The signal can be detected by anti-Biotin Western blotting.

Cells proliferation CCK8 Assay Cells were synchronized in G0 phase by serum deprivation and then released from growth arrest by reexposure to serum, and then cells were grown in complete medium for assay according to the manufacturer

instruction. In brief, cells at a concentration 4×10^3 were seeded into 96-well culture plates in 100 μ l culture medium containing 10% heat-inactivated fetal calf serum(FCS).Before detected, add 10 μ g/well cell proliferation reagent CCK8 and incubate for 4 hours at 37°C and 5% CO₂ .Shake thoroughly for 1 min on shaker. Measure the absorbance of the samples against a background control as blank using a Microplate(ELISA) reader. Each sample was assayed in triplicates at daily intervals after seeding for up to 6 days consecutively. Cell growth curve was based on the corresponding the normalized values of OD450 and each point represents the mean of three independent samples.

Xenograft transplantation in vivo Four-weeks male athymic Balb/C mice were purchased from Shi laike company(Shanghi,China) and maintained in the Tongji animal facilities approved by the China Association for accreditation of laboratory animal care. The athymic Balb/C mouse per group were injected at the armpit area subcutaneously with suspension of 1×10^8 induced hepatocyte-like stem cells in 100 μ l of phosphate buffered saline. The mice were observed 8 weeks, and then sacrificed to recover the tumors. The wet weight of each tumor was determined for each mouse. A portion of each tumor was fixed in 4% paraformaldehyde and embedded in paraffin for histological hematoxylin-eosin(HE) staining. The use of mice for this work was reviewed and approved by the institutional animal care and use committee in accordance with China national institutes of health guidelines.

Supplementary FIGURE LEGENDS

FigureS1 The hepatoblast derived from human ES cells were subjected to transform onto liver cancer in CUDR overexpressed and CCL4 treated injury mouse liver. **A.** The representative analytic results of histological hematoxylin-eosin(HE) staining. A portion of each tumor was fixed in 4% paraformaldehyde and embedded in paraffin for HE staining. **B.** The representative analytic results of immunohistochemical staining. A portion of each tumor was fixed in 4% paraformaldehyde and embedded in paraffin for immunohistochemical staining with anti-AFP.

FigureS2 CUDR overexpression combined with inflammatory factor IL6 produced hepatocyte-like stem cells malignant transformation in *vitro* and in *vivo*. **A.** The schematic illustrates a model of human stem cell line MEL-2 transfected with CUDR overexpression or knockdown plasmids differentiation into hepatoblasts which were further differentiated into hepatocytes-like stem cells. Meanwhile, the hepatoblasts were treated with IL6 till differentiation into hepatocyte-like cells, and the hepatocyte-like stem cells were further treated with IL6 for 10 days. **B.** S phase cells assay using BrdU. Each value was presented as mean±standard error of the mean (SEM), **,P<0.01. **C.** Cells sphere formation ability. **D.** *in vivo* test in induced and treated hepatocytes-like stem cells. The representative analytic results of histological hematoxylin-eosin(HE) staining. A portion of each tumor was fixed in 4% paraformaldehyde and embedded in paraffin for histological hematoxylin-eosin(HE) staining. (original magnification×100).

Figure S3 CUDR enhances SUV39h2 expression in hepatocyte-like stem cells with IL6 treatment. **A.** METTL3 and FTO expression analysis by western blotting with anti-METTL3, anti-FTO. β -actin as internal control. **B.** Super-EMSA(gel-shift) with biotin-SUV39h2 cRNA probe and anti-N6A me antibody. The intensity of the band was examined by western blotting with anti-Biotin. **C.** Nuclear Run on followed by western blotting with anti-N6Ame antibody primer in IL6/12, TNF α

treated hepatocyte-like stem cells transfected with pCMV6-A-GFP,pCMV6-A-GFP-CUDR,pGFP-V-RS,pGFP-V-RS-CUDR. Histone 3 as internal control.

FigureS4 CUDR cooperates with IL6 to enhance NF- κ B expression and phosphorylation. Chromosome conformation capture (3C)-chromatin immunoprecipitation (ChIP) with anti-H3K9me3,anti-RNA polIII in IL6 untreated hepatocyte-like stem cells transfected with pCMV6-A-GFP, pCMV6-A-GFP-CUDR, pGFP-V-RS, pGFP-V-RS-CUDR.The PCR analysis is applied for detecting NF- κ B promoter-enhancer coupling product using NF- κ B promoter and enhancer primers. The NF- κ B promoter and enhancer as INPUT.

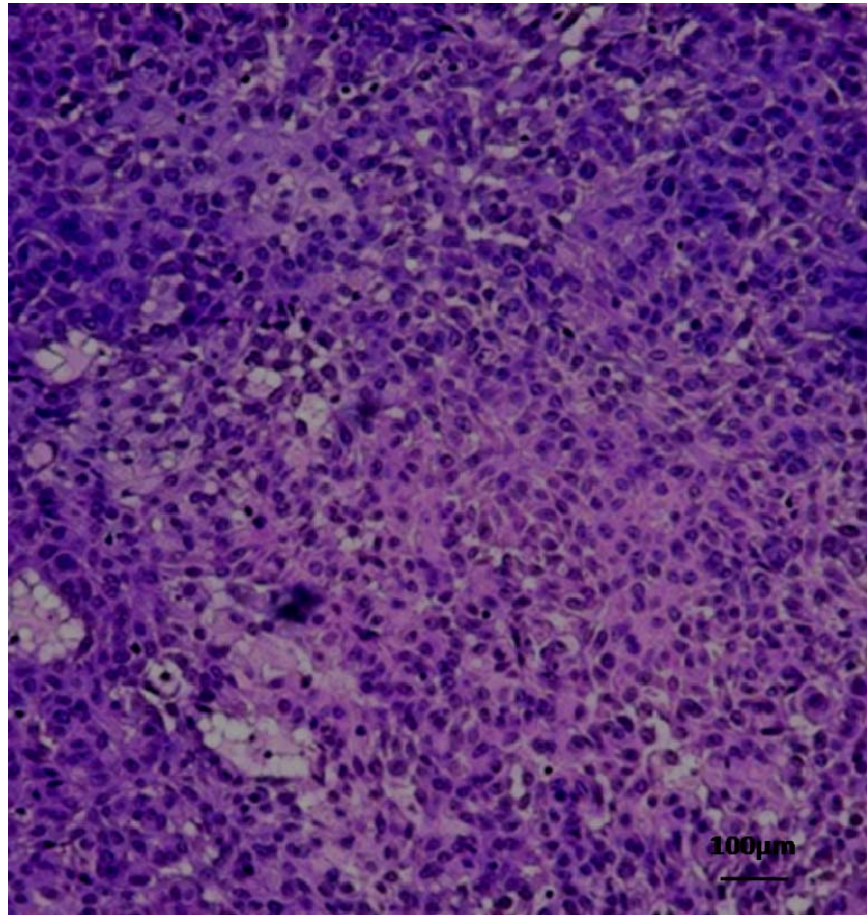
Figure S5 CUDR plus IL6 promotes miRs expression through pStat3 **A.** Chromatin Immunoprecipitation(CHIP) with anti-pStat3 followed by PCR with miR155,miR17,miR675,miR372,miR192 promoter primer in IL6 treated hepatocyte-like cells transfected with pCMV6-A-GFP,pCMV6-A-GFP-CUDR,pGFP-V-RS,pGFP-V-RS-CUDR. IgG CHIP as negative control. miR155,miR17,miR675,miR372,miR192 promoter DNA as INPUT. **B.** Nuclear run on analysis with Biotin probe of miR21,miR155,miR17,miR675,miR372,miR192 in IL6/12,TNF α treated hepatocyte-like cells transfected with pCMV6-A-GFP, pCMV6-A-GFP-CUDR,pGFP-V-RS,pGFP-V-RS-CUDR. β -actin as internal control.

Figure S6 CUDR plus IL6 alters long noncoding RNA expression through pStat3. Chromatin Immunoprecipitation(CHIP) with anti- pStat3 followed by PCR with MEG3, TERRA promoter primer in IL6 treated hepatocyte-like cells transfected with pCMV6-A-GFP,pCMV6-A-GFP-CUDR,pGFP-V-RS,,pGFP-V-RS-CUDR. IgG CHIP as negative control. CUDR,HOTAIR,MALAT1,MEG3,HULC,H19,TERRA promoter DNA as INPUT.

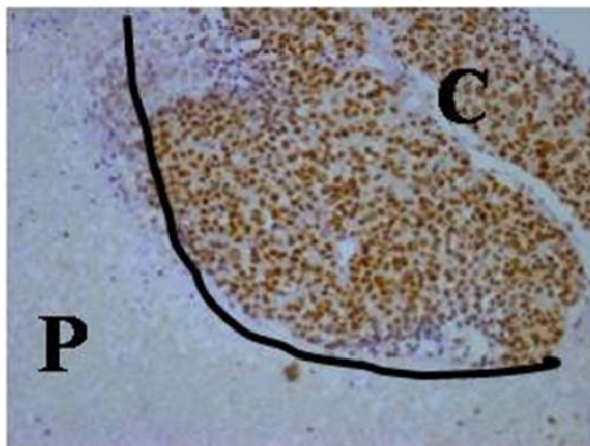
Supplementary FIGURE

FigureS1

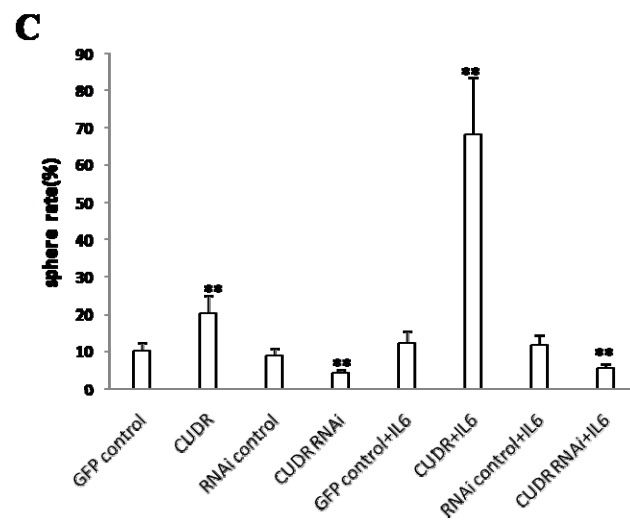
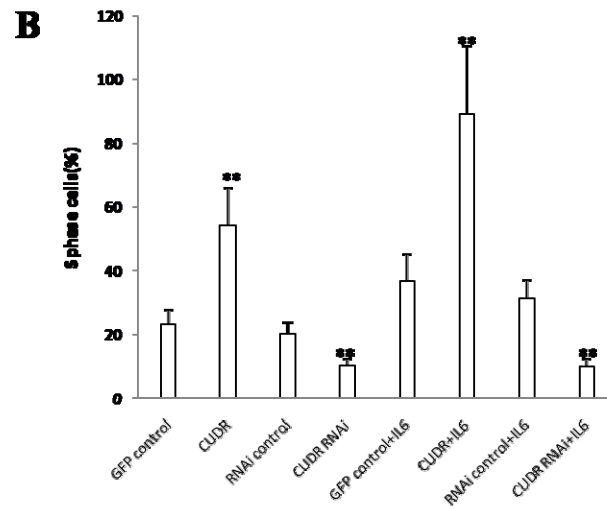
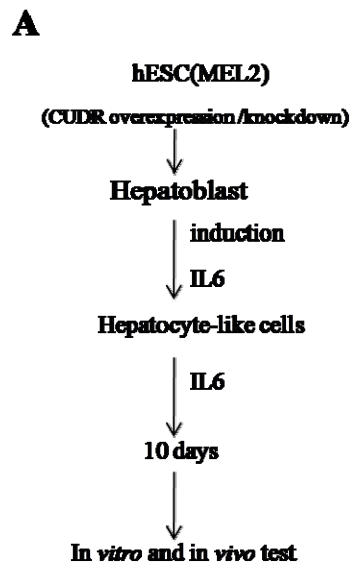
A



B

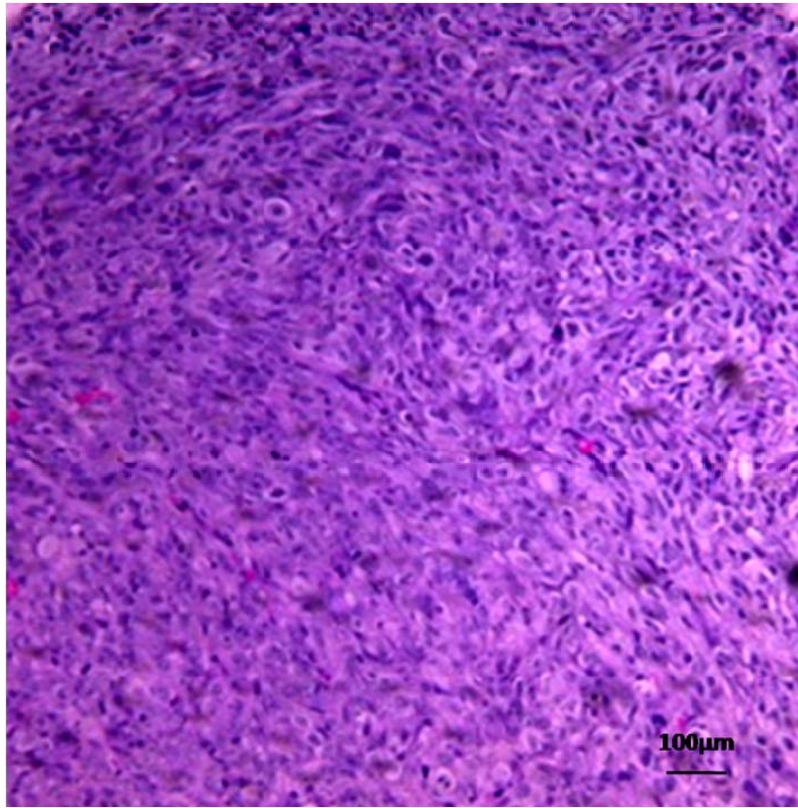


FigureS 2

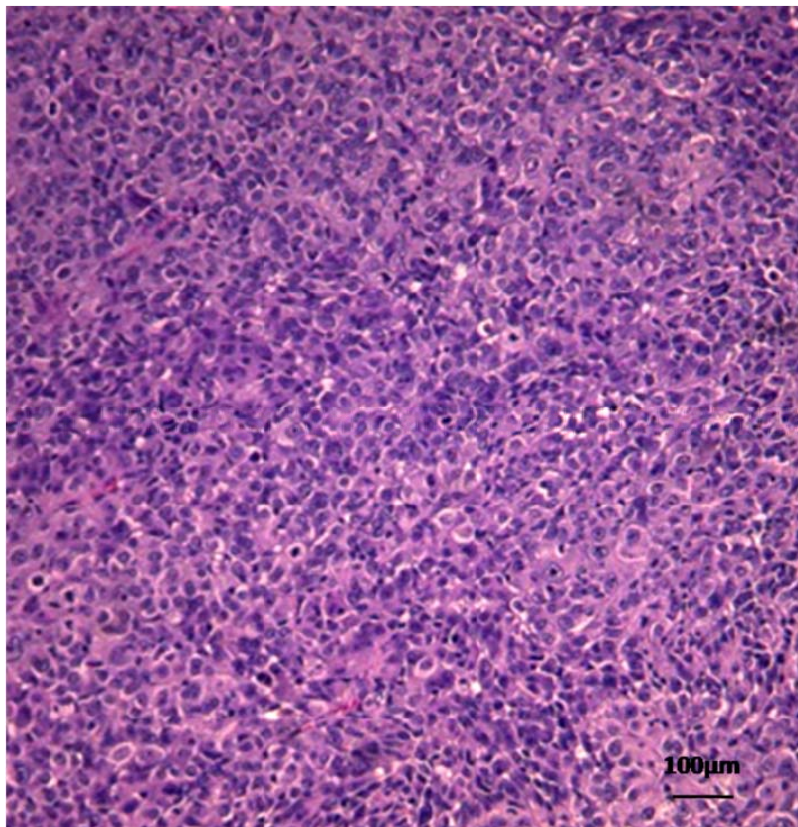


D

Control

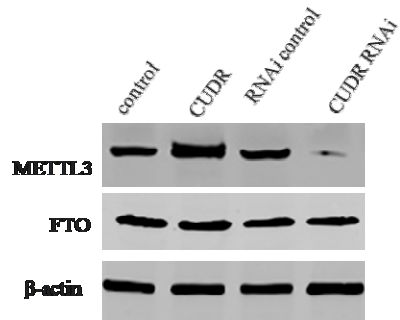


CUDR+IL6

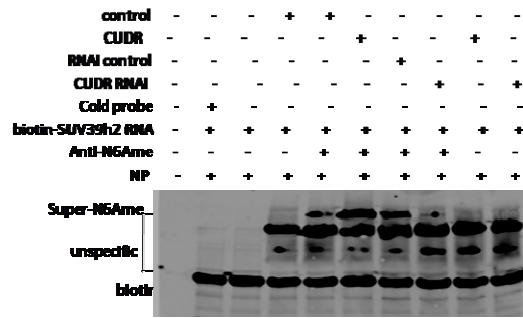


FigureS3

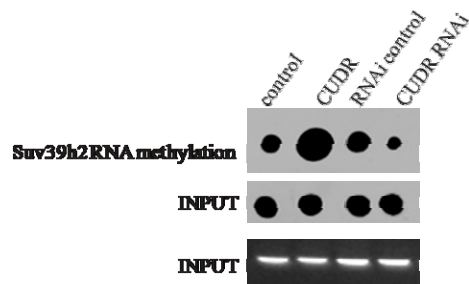
A



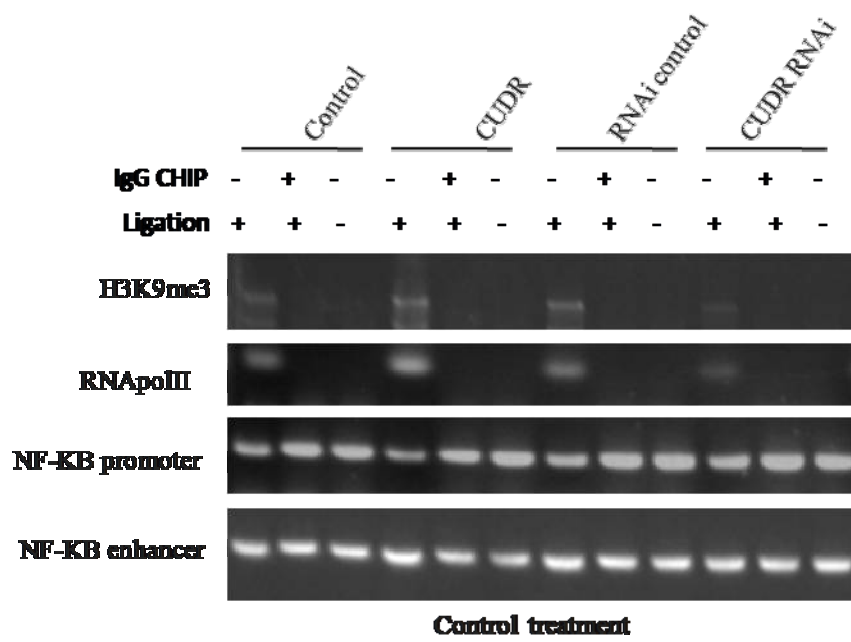
B



C

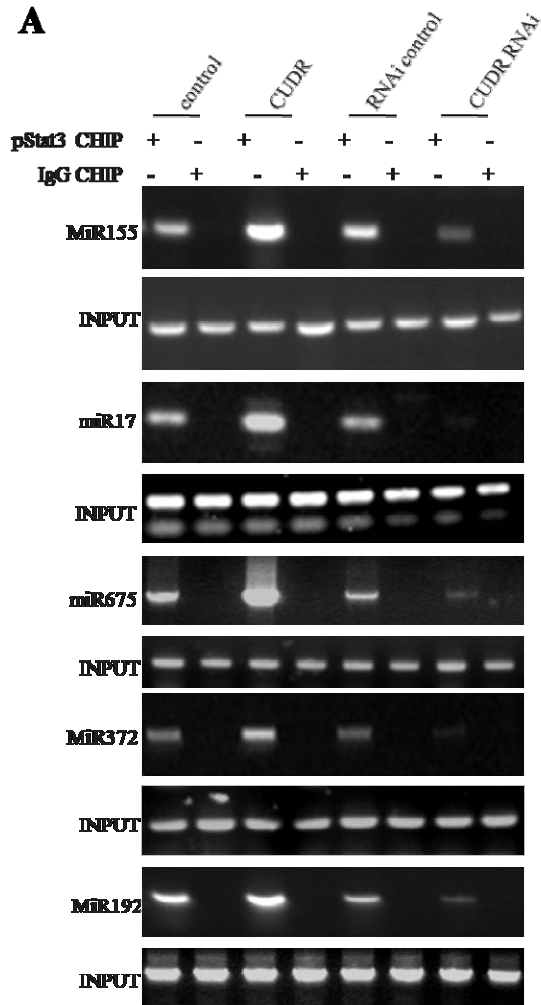


FigureS4

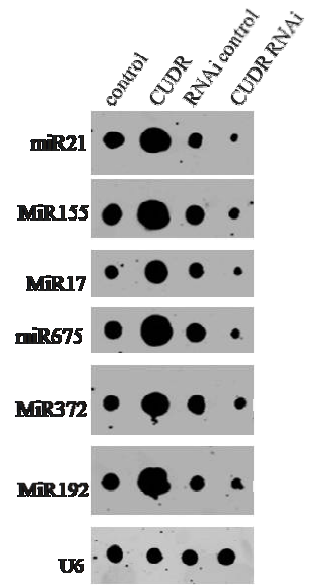


FigureS5

A



B



FigureS6

